*Liquid Crystals Reviews*, 2015
Vol. 3, No. 1, 1–27, http://dx.doi.org/10.1080/21680396.2015.1025305

Taylor & Francis
Taylor & Francis Group

# The nature of the assembly process in chromonic liquid crystals

Peter J. Collings[a,b*], Joshua N. Goldstein[a], Elizabeth J. Hamilton[a], Benjamin R. Mercado[a], Kenneth J. Nieser[a] and Margaret H. Regan[a]

[a]*Department of Physics and Astronomy, Swarthmore College, Swarthmore, PA 19081, USA;* [b]*Department of Physics and Astronomy, University of Pennsylvania, Philadelphia, PA 19104, USA*

(*Received 27 February 2015; accepted 27 February 2015*)

Chromonic liquid crystals form when certain molecules are dissolved in a solvent, usually water, and the molecules spontaneously assemble into anisotropic structures. If the density of these structures is high enough and the temperature is low enough, they organize into a liquid crystal phase with orientational and sometimes with positional order also. Chromonic liquid crystals have been studied for more than half a century, yet theoretical, computational, and experimental investigations in the last decade have revealed many more details about them. The molecular structures that form chromonic liquid crystals are quite varied, and as a result the assemblies that these molecules form vary significantly also. Recent research has begun to shed light on these assembly processes, revealing that these too can be quite different from one system to another.

**Keywords:** chromonic; liquid crystal; lyotropic; molecular assembly; assembly kinetics



## 1. Introduction

The story of chromonic liquid crystals normally starts with the work of Sandquist in 1915 on solutions of phenanthrene sulfonic acid, in which he describes optical textures under a polarizing microscope that reveal the existence of a liquid crystal phase.[1] Reports of other scientists continue in the years after, but independent work by Jelley [2,3] and Schiebe [4] on pseudoisocyanine chloride (PIC) brought significantly more attention to the idea of molecular assembly. Researchers working to understand the efficacy of a new asthma drug initiated the more recent work on chromonics when they published X-ray and optical data on disodium cromoglycate (DSCG).[5] It did not take long before people realized that the two liquid crystal phases identified in this work were composed of columns of stacked molecules.[6] During this period, other chromonic systems were discovered, including some azo dyes,[7] xanthone derivatives,[8,9] and cyanine dyes.[10] Soon thereafter it was realized that work on some nucleic acids revealed similar behavior. An extensive review of all of this work was written by Lydon in 1998.[11] More recent reviews describe what has been learned since that time and together do an excellent job of covering the entire field.[12–17]

It was realized fairly early that the assembly process that formed the columns of stacked molecules is close to isodesmic, meaning that the change in free energy for a molecule joining the stack is nearly independent of the number of molecules in the stack.[11] This means molecules begin to associate at extremely low concentrations, with the numbers and average size ofthe assemblies increasing as the concentration increases. In particular, there is no threshold at which assembly formation begins as is the case with the formation of micelles in amphiphilic systems. The onset of liquid crystallinity critically depends on the size and density of assemblies, so it appears as a phase transition, although a wide coexistence region, on the order of 10 K, is usually present. The formation of a liquid crystal phase at room temperature for systems undergoing isodesmic assembly occurs when the concentration is typically between 10 and 30 wt%. However, there are numerous reports in the literature that some systems behave differently, forming a liquid crystal phase at much lower concentrations (typically below 1 wt%), with indications that a threshold for assembly might be present. These include PIC,[18] cyanine dyes,[10,19] an azo dye,[10] benzopurpurin 4B,[20,21] and more recently pinacyanol acetate [22] and IR-806.[23] The working hypothesis is that the assembly structure is more complex and contains water, allowing these larger assemblies to interact and form a liquid crystal phase at significantly lower concentrations.

This review focuses on the assembly process in systems that form chromonic liquid crystals. Molecular assembly is common in nature and is responsible for a wide range of phenomena in fields such as material science and biology, just to name two. While significant scientific research has shed light on the assembly process in many systems, such is not the case for the compounds that form liquid crystal phases. Most of the work on chromonic liquid crystals has

*Corresponding author. Email: pcollin1@swarthmore.edu

been devoted to understanding either the structure of the assemblies or the properties of the liquid crystal phases. It is the research that has revealed information about the assembly process that is described here. Most of this work is quite recent and includes theoretical, computational, and experimental investigations. It has also been aided by efforts to image the assemblies using cryo-transmission electron microscopy.[24,25]

## 2. Simple models of assembly

It is worthwhile to begin a discussion of the models of the assembly process with the most simple ones. There are two reasons for this. First, more complex assembly models are in some senses extensions of the simple models. Second, in the case of chromonic liquid crystals, the simple models correspond to what is observed in some cases. Typically, models of assembly are described either through a series of reactions or by determining the partition function of the system. The former is used in this review, but general references that describe each of them are available.[26,27]

### 2.1. Isodesmic assembly

In the isodesmic assembly model, the change in the free energy for the addition or subtraction of a molecule from an assembly is independent of the size of the assembly. This can be described by a series of chemical reactions, all of which involve one molecule and an assembly, but with the equilibrium constant the same for all reactions.

$$\begin{aligned} A_1 + A_1 &\rightleftharpoons A_2, \quad K = \frac{[A_2]}{[A_1]^2}, \\ A_2 + A_1 &\rightleftharpoons A_3, \quad K = \frac{[A_3]}{[A_2][A_1]}, \\ &\vdots \qquad\qquad \vdots \\ A_{i-1} + A_1 &\rightleftharpoons A_i, \quad K = \frac{[A_i]}{[A_{i-1}][A_1]}. \end{aligned} \tag{1}$$

Here $A_1$ represents a single molecule, $A_i$ represents an assembly of $i$ molecules, $K$ is the equilibrium constant for all of the reactions, and the brackets denote concentrations. The system is constrained because the number of single molecules in solution plus the number of molecules in assemblies of any size must add up to the total number of molecules in the system. If $C_T$ is the total concentration of molecules in the system and if $C_i = [A_i]$ is the concentration of assemblies of size $i$, then the following equation describes the constraint.

$$\begin{aligned} C_T &= C_1 + \sum_{i=2}^{\infty} iC_i = C_1 + \sum_{i=2}^{\infty} iKC_{i-1}C_1 \\ &= \frac{1}{K}\sum_{i=1}^{\infty} i(KC_1)^i. \end{aligned} \tag{2}$$

After performing the summation with $KC_1 < 1$, this yields

$$KC_T = \frac{KC_1}{(1-KC_1)^2}, \tag{3}$$

which results in a quadratic equation with the following solution for $C_1$ and $\alpha_1$, the fraction of single molecules in solution.

$$\begin{aligned} C_1 &= \frac{2KC_T + 1 - \sqrt{4KC_T + 1}}{2K^2C_T} \quad \text{and} \\ \alpha_1 &= \frac{C_1}{C_T} = \frac{2KC_T + 1 - \sqrt{4KC_T + 1}}{2(KC_T)^2}. \end{aligned} \tag{4}$$

The concentration of the assemblies of different sizes and the fraction of molecules in each size of assembly, $\alpha_i$, are then

$$C_i = K^{i-1}C_1^i \quad \text{and} \quad \alpha_i = \frac{iC_i}{C_T} = \frac{i(KC_1)^i}{KC_T} = i(KC_T)^{i-1}\alpha_1^i. \tag{5}$$

Notice how convenient it is to work with the fractions of molecules in each size of assembly, since they depend only on the product of $K$ and $C_T$ because $KC_1$ depends only on product of $K$ and $C_T$. How some of the fractions depend on $C_T$ is shown in Figure 1, where several $\alpha_i$ are plotted against $KC_T$. Note also that the concentration of assemblies of different size $C_i$ is an exponential function of $i$ with a characteristic size of $-1/\ln(KC_1)$.

As is evident from Figure 1(a), the formation of assemblies is a continuous process. A small number of small assemblies form at extremely low concentration, and the number and average size of the assemblies increase as the concentration increases. There is no threshold concentration for assembly formation.

### 2.2. Cooperative assembly

In isodesmic assembly, molecules are added or subtracted from an assembly one at a time. There are no interactions between molecules not already in the assembly during the addition process, and no interactions between molecules in the assembly during the subtraction process. This contrasts to cases in which more than one molecule is involved in creating or destroying an assembly, the simplest being when a specific number of molecules is necessary to form an assembly. Such a process is called "cooperative", because interactions between the molecules play a necessary role. Perhaps the best example of such a process is the formation of micelles in amphiphilic systems. Only full, spherical micelles form, meaning that all assemblies contain a specific number of molecules.

The case in which all assemblies have $N$ molecules is particularly easy to model. There are only two species present, a molecule $A_1$ and an assembly $A_N$, only one

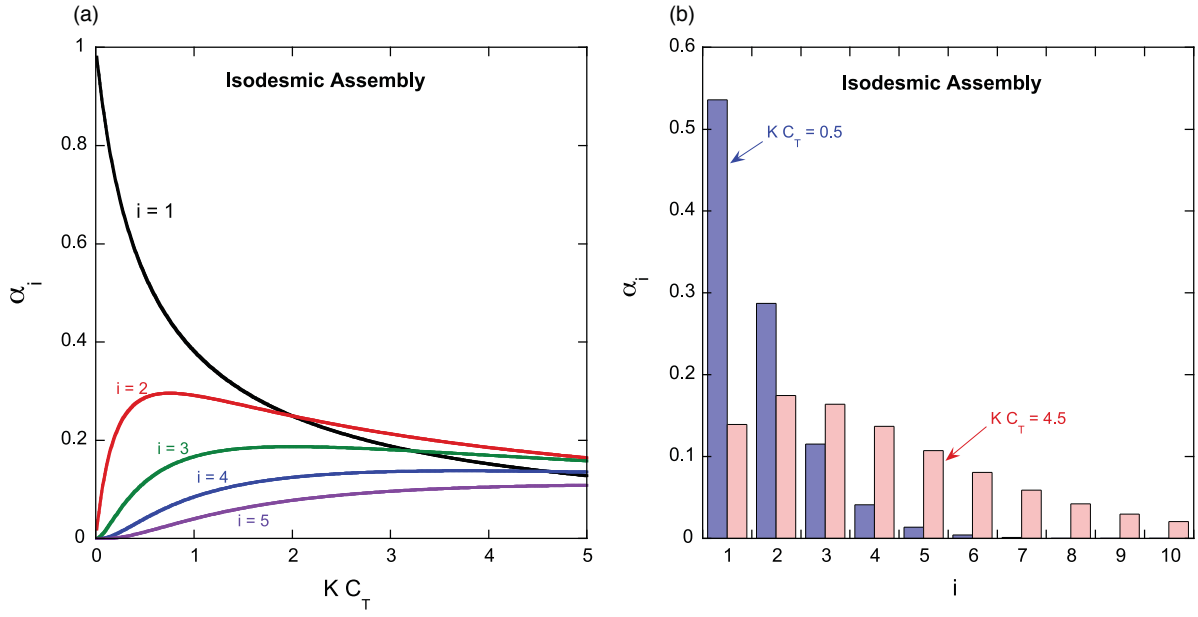


Figure 1. (a) Fraction of molecules in different sizes of assemblies $\alpha_i$ versus the equilibrium constant times the total concentration of molecules, $KC_T$, for isodesmic assembly. The size of the assembly is given by the number of molecules in it, $i$. Since $K$ is a constant, the $KC_T$ axis can be thought of as the $C_T$ axis. (b) Fraction of molecules in different sizes of assemblies $\alpha_i$ versus the size of the assembly $i$ for two values of $KC_T$.

reaction, and one constraint.

$$NA_1 \rightleftharpoons A_N, \quad K_N = K_E^{N-1} = \frac{[A_N]}{[A_1]^N},$$
$$C_T = C_1 + NC_N, \tag{6}$$

where $C_N = [A_N]$ is the concentration of assemblies of size $N$. Combining the two equations results in a $N$th order equation that needs to be solved, which can be simplified by multiplying each term by $K_E$.

$$K_E C_T = K_E C_1 + N(K_E C_1)^N. \tag{7}$$

Rather than solving the $N$th order equation, one can specify values for $N$ and $K_E C_1$, use them to calculate $K_E C_T$, and then find $\alpha_1$ and $\alpha_N$ from the following relations.

$$\alpha_1 = \frac{K_E C_1}{K_E C_T} \quad \text{and} \quad \alpha_N = \frac{K_E C_T - K_E C_1}{K_E C_T}. \tag{8}$$

The results of such calculations are shown in Figure 2, where both $\alpha_1$ and $\alpha_N$ are plotted as a function of $K_E C_T$. Notice how the assembly process gets more and more abrupt as $N$ increases, approaching a discontinuity in the slope at $K_E C_T = 1$ as $N \to \infty$. Since all of the processes shown in Figure 2 involve $N > 2$, they are all cooperative; the ones with large values of $N$ represent highly cooperative assembly processes.

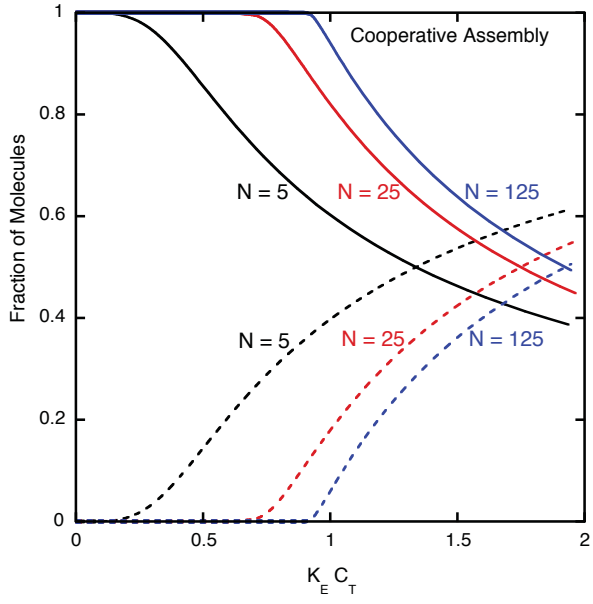


Figure 2. Fraction of single molecules, $\alpha_1$ (solid lines), and fraction of molecules in assemblies of size $N$, $\alpha_N$ (dashed lines), versus $K_E C_T$ for various values of $N$ in a simple model of cooperative assembly. Notice how the threshold in the assembly process gets more and more abrupt as $N$ increases.

## 3. More complicated models of assembly

The typical way assembly models become more complicated is by combining simple models. If an assembly process consists of two steps in which the first step must occur before the second step happens, then it usually can be modeled by having a simple model describing each step. Three examples of such two-step models are described in this section.

### 3.1. *Quasi-isodesmic assembly*

The experimental evidence for some systems is that the formation of an assembly of two molecules is governed by one equilibrium constant, while adding a molecule to an assembly of two or more molecules is described by a different equilibrium constant. This results in the following reactions and equations, where $K_2 = \rho K$ is the equilibrium constant for two molecules forming an assembly and $K$ is the equilibrium constant for adding a molecule to assemblies of two or more molecules.

$$\begin{aligned} &A_1 + A_1 \rightleftharpoons A_2, \quad K_2 = \frac{[A_2]}{[A_1]^2}, \\ &A_2 + A_1 \rightleftharpoons A_3, \quad K = \frac{[A_3]}{[A_2][A_1]}, \\ &\vdots \qquad\qquad\qquad \vdots \\ &A_{i-1} + A_1 \rightleftharpoons A_i, \quad K = \frac{[A_i]}{[A_{i-1}][A_1]}. \end{aligned} \tag{9}$$

The constraint equation can be written as follows :

$$\begin{aligned} C_T &= C_1 + \rho \sum_{i=2}^{\infty} iK^{i-1}C_1^i, \\ KC_T &= \rho \sum_{i=1}^{\infty} i(KC_1)^i + (1-\rho)KC_1 \\ &= \frac{\rho KC_1}{(1-KC_1)^2} + (1-\rho)KC_1. \end{aligned} \tag{10}$$

Again, instead of solving a cubic equation for $C_T$, one can start with values for $\rho$ and $KC_1$, generate a value for $KC_T$, and determine the value of $\alpha_1 = KC_1/KC_T$. Knowing $\alpha_1$, the values for $\alpha_i$ can be found using Equation (9), that is, $KC_i = \rho(KC_1)^i$ or $\alpha_i = iKC_i/KC_T = i\rho(KC_1)^i/KC_T$. One can see how this assembly process works by looking at Figure 3. If $\rho < 1$, the formation of assemblies of two molecules is the rate-limiting step and threshold-like behavior can be present (the smaller $\rho$ is, the sharper the threshold). The fractions of molecules in different sizes of assemblies are not shown in Figure 3 because they are quite small, that is, the distribution of assembly sizes is very broad.

### 3.2. *Activation and growth assembly*

Another model with the potential for a rate-limiting initial reaction is the activation and growth model. Here the first step of the assembly process is the change of a molecule to an activated state before it can join, one molecule at a time, with other activated molecules or assemblies. One example of such activation is a conformational change that is necessary for molecules to form weak bonds with each other. Normally, the addition of activated molecules to already formed assemblies is assumed to be isodesmic. The

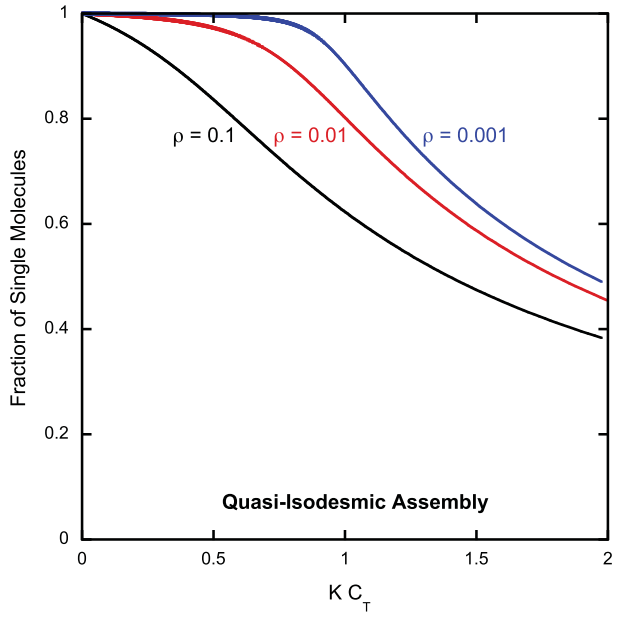


Figure 3. Fraction of single molecules, $\alpha_1$ versus $KC_T$ for various values of $\rho$ in a quasi-isodesmic assembly process. Notice how the threshold-like behavior in the assembly process gets sharper as $\rho$ decreases.

reactions involved are therefore as follows, with activated molecules denoted with an asterisk and $K_A$ the equilibrium constant for the activation reaction.

$$\begin{aligned} &A_1 \rightleftharpoons A_1^*, \quad K_A = \frac{[A_1^*]}{[A_1]}, \\ &A_1^* + A_1^* \rightleftharpoons A_2^*, \quad K = \frac{[A_2^*]}{[A_1^*]^2}, \\ &A_2^* + A_1^* \rightleftharpoons A_3^*, \quad K = \frac{[A_3^*]}{[A_2^*][A_1^*]}, \\ &\vdots \qquad\qquad\qquad \vdots \\ &A_{i-1}^* + A_1^* \rightleftharpoons A_i^*, \quad K = \frac{[A_i^*]}{[A_{i-1}^*][A_1^*]}. \end{aligned} \tag{11}$$

As before, the concentrations of the assemblies can be expressed in terms of the concentration of unactivated molecules and the two equilibrium constants, yielding a slightly different constraint equation.

$$\begin{aligned} C_T &= C_1 + \sum_{i=1}^{\infty} iK_A^i K^{i-1} C_1^i, \\ K_A KC_T &= K_A KC_1 + \frac{K_A(K_A KC_1)}{(1-K_A KC_1)^2}. \end{aligned} \tag{12}$$

For computational ease, values for $K_A$ and $K_A KC_1$ are first specified, then $K_A KC_T$ is calculated from Equation (12), after which the fractions of unactivated, activated, and assemblies of activated molecules ($\alpha_1, \alpha_1^*$, and $\alpha_i^*$, respectively) can be determined as before. Figure 4 shows a plot

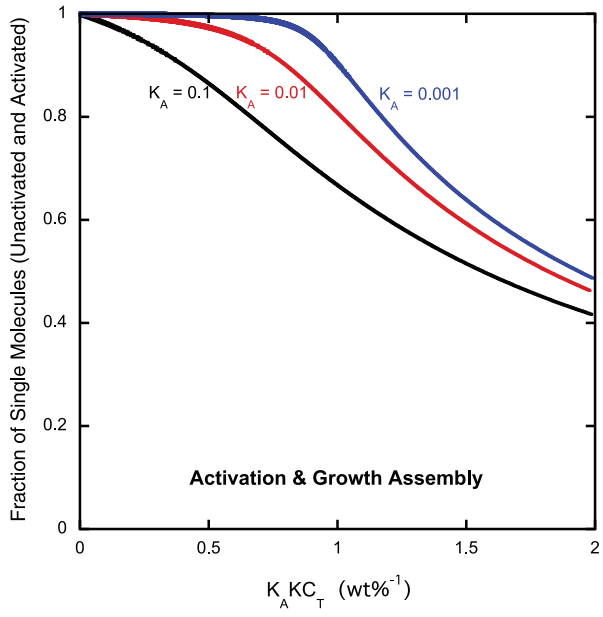


Figure 4. Fraction of single molecules (unactivated $\alpha_1$ and activated $\alpha_1^*$) versus $K_A KC_T$ for various values of $K_A$ in an activation and growth assembly process. Notice how the threshold-like behavior in the assembly process gets sharper as $K_A$ decreases.

of the fraction of single molecules (unactivated and activated) as a function of $K_A KC_T$. It is interesting to note that a small equilibrium constant for the activation reaction produces the same type of effect as a small equilibrium constant for the first reaction in an otherwise isodesmic assembly process, that is, compare Figures 3 and 4. In fact, these two models have been shown to be nearly equivalent in general and exactly equivalent when the equilibrium constant for the initial reaction is much, much less than the growth equilibrium constant.[28]

### 3.3. *Nucleation and growth assembly*

In the nucleation and growth assembly process, the first reaction is $N$ molecules coming together to form an assembly with an equilibrium constant $K_N$. Single molecules can join an assembly of $N$ or more molecules in a reaction governed by an equilibrium constant $K$. As with the activation and growth model, the addition of single molecules to assemblies is usually assumed to be isodesmic. With these assumptions, the equilibrium reactions take slightly different forms.

$$\begin{aligned}
&NA_1 \rightleftharpoons A_N, \quad C_N = K_N C_1^N,\\
&A_N + A_1 \rightleftharpoons A_{N+1}, \quad C_{N+1} = KC_N C_1 = KK_N C_1^{N+1},\\
&A_{N+1} + A_1 \rightleftharpoons A_{N+2}, \quad C_{N+2} = KC_{N+1} C_1 = K^2 K_N C_1^{N+2},\\
&A_{N+2} + A_1 \rightleftharpoons A_{N+3}, \quad C_{N+3} = KC_{N+2} C_1 = K^3 K_N C_1^{N+3},\\
&\vdots \qquad\qquad \vdots \qquad\qquad (13)\\
&A_{N+i-1} + A_1 \rightleftharpoons A_{N+i}, \quad C_{N+i} = KC_{N+i-1} C_1 = K^i K_N C_1^{N+i}.
\end{aligned}$$

The constraint equation is different also.

$$C_T = C_1 + \sum_{i=0}^{\infty} (N+i) C_{N+i} = C_1 K_N C_1^N \sum_{i=0}^{\infty} (N+i) K^i C_1^N. \tag{14}$$

After performing the summation and letting $\sigma$ be defined by $K_N = \sigma K^{N-1}$, this yields

$$C_T = C_1 + \sigma \frac{(KC_1)^N}{K} \frac{N - (N-1)KC_1}{(1 - KC_1)^2}. \tag{15}$$

Given values for the parameters $C_T$, $N$, $K$, and $\sigma$, the concentration of molecules $C_1$ can be calculated. The concentrations of assemblies of all the other sizes can then be calculated using Equation (13). Again, solving Equation (15) involves an equation of $N$th order. A more simple way to perform the calculation is to multiply both sides of Equation (15) by $K$,

$$KC_T = KC_1 + \sigma (KC_1)^N \frac{N - (N-1)KC_1}{(1 - KC_1)^2}. \tag{16}$$

First a value for $KC_1$ is chosen. Then, Equation (16) is used to calculate $KC_T$. Finally, the fraction of single molecules $\alpha_1 = KC_1/KC_T$ and the fraction of molecules in all of the assemblies $\alpha_N = 1 - \alpha_1 = (KC_T - KC_1)/KC_T$ are determined. Instead of graphing $\alpha_1$, the fraction of molecules in assemblies, $\alpha_N$, is plotted versus $KC_T$ in Figure 5 for a fixed value of $\sigma$ and a wide range of nucleus sizes $N$. Notice that as the nucleus size increases, the onset of assembly formation gets more abrupt. In the limit of infinite nucleus size, the plot would have a discontinuous slope at $KC_T = 1$. It

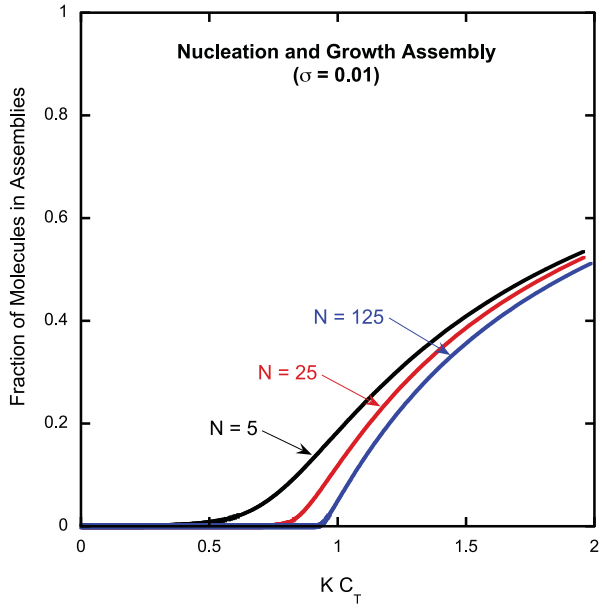


Figure 5. Fraction of molecules in assemblies versus $KC_T$ for various values of $N$ in a nucleation and growth assembly process with $\sigma = 0.01$. The threshold-like behavior in the assembly process gets sharper as $N$ increases.

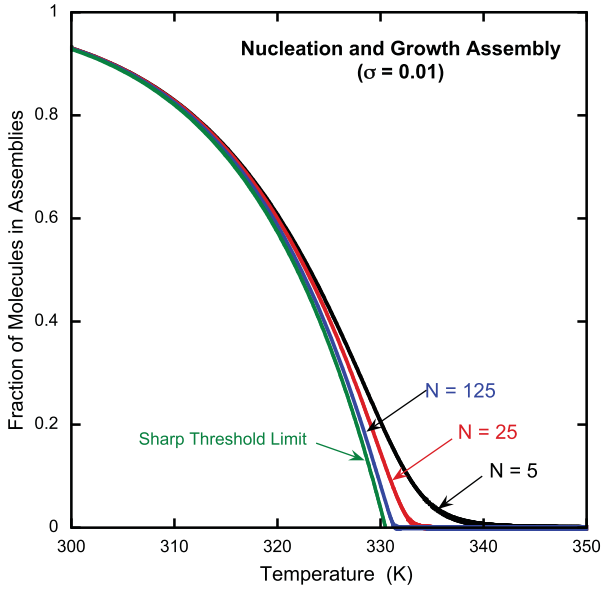


Figure 6. Fraction of molecules in assemblies versus temperature for various values of $N$ in a nucleation and growth assembly process with $\sigma = 0.01$ and $C_T = 0.2$ wt% as explained in the text. The abruptness of the threshold-like behavior in the assembly process increases as $N$ increases. The sharp threshold limit plot is more general and is discussed in the text.

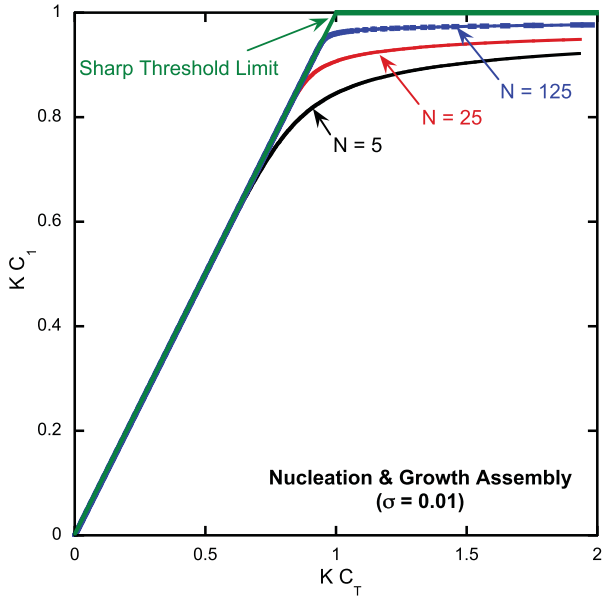


Figure 7. $KC_1$ versus $KC_T$ for various values of the nucleus size $N$ in the nucleation and growth assembly model with $\sigma = 0.01$. The sharp threshold limit is for $N \to \infty$, for which $KC_1 = 1$ if $KC_T > 1$.

should be pointed out that the same progression toward a more abrupt threshold results if $N$ remains constant and $\sigma$ is decreased.

So far the discussion of all the models has been for constant temperature. It is important to understand how temperature enters into a model, and the nucleation and growth model can be used to illustrate this. If one assumes that the growth equilibrium constant $K$ depends on the absolute temperature $T$ as follows:

$$K = K_0\, e^{-\Delta G/RT}, \tag{17}$$

where $\Delta G$ is a Gibbs free energy change, $R$ is the gas constant, and $K_0$ is the proportionality constant, then plots showing how the fraction of molecules in assemblies depends on temperature can be generated for a specified total concentration $C_T$. An easy way to do this is to specify $KC_1$, determine $KC_T$ using Equation (16), then calculate $\alpha_N$, and finally pair these values with a temperature $T = (-\Delta G/R)/\ln(K/K_0)$. Such plots are shown in Figure 6, where the various parameters have been chosen so the process occurs over a suitable range of temperatures near room temperature ($C_T = 0.2$ wt%, $\Delta G/R = -8600$ K, and $K_0 = 2.5 \times 10^{-11}$ wt%$^{-1}$). Notice again that the assembly process begins more and more abruptly with decreasing temperature as the size of the nucleus increases.

### 3.4. *Sharp threshold limit*

Instead of plotting the fractions of molecules that are either single $\alpha_1$ or in assemblies $\alpha_N$, it is instructive to look at how $KC_1$ depends on $KC_T$ as $N$ is varied in the nucleation and growth model. This is shown in Figure 7, where it is clear that in the limit of an extremely sharp threshold, $KC_1 = 1$ for values of $KC_T$ above the threshold value of $KC_T = 1$.

Thus, Equation (17) indicates that there is a threshold temperature $T^*$, with $K_0\, e^{-\Delta G/(RT^*)} C_T = 1$, above which there are no assemblies. If $T < T^*$, then $\alpha_N = 1 - \alpha_1 = 1 - (1/KC_T)$. Substituting $K$ from Equation (17) into this expression and using the definition of $T^*$ yield an expression for the fraction of molecules in assemblies as a function of $T$, originally formulated by van der Schoot.[29]

$$\alpha_N = 1 - \alpha_1 = 1 - \exp\left[\left(\frac{-\Delta G}{R}\right)\left(\frac{1}{T^*} - \frac{1}{T}\right)\right] \qquad T < T*. \tag{18}$$

This sharp threshold limit is shown in Figures 6 and 7.

## 4. Kinetics of the assembly models

The easiest kinetics experiment to perform on chromonic liquid crystal systems is to start with a solution in which there are assemblies in equilibrium and quickly cause a decrease in concentration by diluting with water. Since the system is no longer in equilibrium, the concentrations of single molecules and the different sizes of assemblies will change, eventually reaching an equilibrium condition appropriate to the new concentration. Another similar

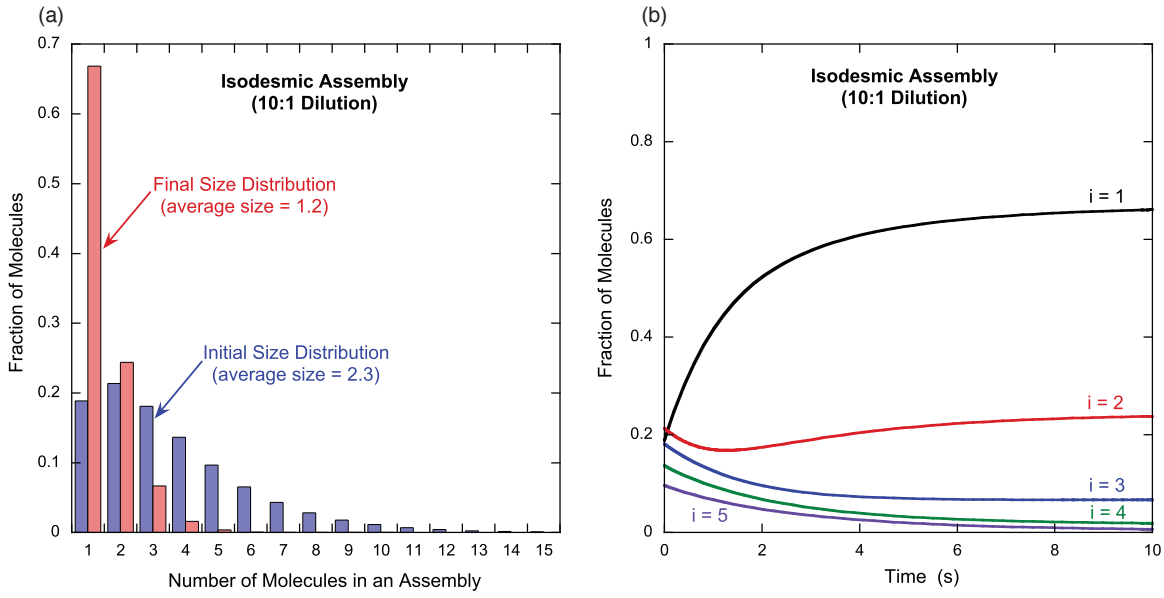


Figure 8. Kinetics of a dilution for the isodesmic assembly model. (a) Distribution of assembly sizes both before ($C_T = 0.300$ wt%) and after ($C_T = 0.300$ wt%/11 = 0.027 wt%) a 10:1 dilution ($K = 10\,\text{wt\%}^{-1}$). (b) The time dependence of the distribution of assembly sizes immediately after dilution for the five smallest assembly sizes ($k_+ = 10$ (wt% s)$^{-1}$, $k_- = 1\,\text{s}^{-1}$). The number of molecules in an assembly is given by $i$.



experiment is to subject a solution in equilibrium to a sudden increase in temperature. This changes the equilibrium constants and therefore forces the solution to adopt the molecular and assembly concentrations dictated by the new equilibrium constants. Finally, kinetics experiments can be done by rapidly changing the solvent conditions, which is another way to alter the equilibrium constants. A good example for chromonic liquid crystal systems is to add salt to the solution, which causes the equilibrium constants to change much as a change in temperature does. Since the dilution experiments are the easiest, a few examples of what theory predicts are discussed for this type of experiment.

In the case of isodesmic assembly, the starting point is an equilibrium distribution of assemblies, with each assembly of size $i$ having an initial concentration $C_i(0)$. Then, a set of differential equations is written to reflect how a concentration $C_i(t)$ can increase and decrease. In general, there are four terms in each equation, representing two addition reactions with rate constant $k_+$ and two subtraction reactions with rate constant $k_-$. The two forward reactions either increase or decrease $C_i(t)$, as is also true for the two reverse reactions. If an assembly of size $M$ is the largest to be considered in the calculation, then $C_M(t)$ can only change due to the addition of a molecule to an assembly of $M-1$ molecules or the subtraction of a molecule from an assembly of size $M$. In addition to these differential equations, there is the constraint relationship regarding the total concentration of molecules in the system. These equations are sometimes referred to as the master equations, which usually must be solved numerically given the initial concentrations $C_i(0)$.[30–32]

$$\begin{aligned}
\frac{\mathrm{d}C_i}{\mathrm{d}t} &= k_+C_1C_{i-1} - k_+C_1C_i + k_-C_{i+1} - k_-C_i \\
&\qquad 2 \le i \le M-1, \\
\frac{\mathrm{d}C_M}{\mathrm{d}t} &= k_+C_1C_{M-1} - k_-C_M, \\
\frac{\mathrm{d}C_1}{\mathrm{d}t} &= -\sum_{i=2}^{M} i\frac{\mathrm{d}C_i}{\mathrm{d}t}.
\end{aligned} \tag{19}$$

As an illustration of such a calculation, consider a system at equilibrium with the distribution of assembly sizes given in Figure 8(a) (the average assembly size is 2.3). Imagine the system is then diluted with 10 times as much water, meaning that the concentrations $C_i(t)$ are 11 times less. Solving the master equations shows how the $C_i(t)$ change to a new equilibrium with the distribution of assembly sizes given in Figure 8(a) (the average assembly size is 1.2). The kinetics of the change for the five smallest assembly sizes are shown in Figure 8(b), where the large increase in single molecules and the decrease in larger assembly sizes are evident.

To illustrate the reverse kinetics, that is, assembly formation, the calculation starts with the equilibrium distribution of assembly sizes for the final state of the previous calculation. Then, the master equations are solved for the condition in which the forward rate constant is 11 times larger, which results in an equilibrium distribution of assembly sizes equal to the starting state of the previous calculation. This is shown in Figure 9.

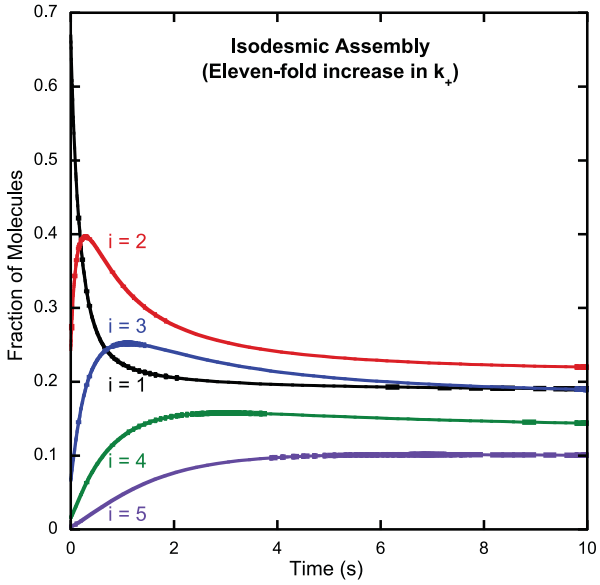


Figure 9. Kinetics of assembly for the isodesmic assembly model. The initial distribution of assembly sizes corresponds to $C_T = 0.300\,\text{wt\%}/11 = 0.027\,\text{wt\%}$ and $K = k_+/k_- = 10\,\text{wt\%}^{-1}$. The master equations are then solved with $k_+$, and therefore $K$, increased by a factor of 11. The final distribution of assembly sizes is the same as the initial assembly size distribution of Figure 8.

An illustration of the kinetics for a more complex model is also enlightening. The set of master equations is more complicated, but still entails a number of differential equations plus the constraint relationship. For the nucleation and growth assembly model with $N$ molecules in the nucleus, the master equations take the following form.

$$\begin{aligned}
\frac{dC_i}{dt} &= 0 \quad 2 \le i \le N-1,\\
\frac{dC_N}{dt} &= k_{N+}C_1^N - k_{N-}C_N - k_+C_1C_N + k_-C_{N+1},\\
\frac{dC_i}{dt} &= k_+C_1C_{i-1} - k_+C_1C_i + k_-C_{i+1} - k_-C_i\\
&\qquad N+1 \le i \le M-1,\\
\frac{dC_M}{dt} &= k_+C_1C_{M-1} - k_-C_M,\\
\frac{dC_1}{dt} &= -\sum_{i=N}^{M} i\frac{dC_i}{dt}.
\end{aligned} \tag{20}$$

Here forward and reverse rate constants, $k_{N+}$ and $k_{N-}$, have been introduced for the first reaction given in Equation (13).

As two examples of kinetics calculations for the nucleation and growth assembly process, consider a 10:1 dilution of a system with a distribution of assembly sizes. Of course, the initial concentration and all the rate constants must be specified, but as before, the initial distribution of assembly sizes is first determined, with these being used as the initial concentrations after being divided by the dilution factor. Figure 10(a) shows the result of such a calculation for different beginning total concentrations. In all cases, the system initially starts with some of the molecules in assemblies and the 10:1 dilution is enough to ensure that at the end, there are no molecules in assemblies. Notice that for the rate constants chosen, the kinetics speed up as the total concentration decreases. This makes sense since the average size of the initial assemblies decreases as the total concentration decreases. Also shown in Figure 10(b) is what happens when the two forward rate constants, $k_{N+}$ and $k_+$, are increased by a factor of 2.5. For the three concentrations in the figure, the initial condition has no molecules in assemblies, but after the rate constants are increased, assemblies start to form, ending up with both single molecules and assemblies. The kinetics are faster, the higher the concentration.

The kinetics for the nucleation and growth model are extremely interesting because the reaction rates for the nucleation reaction and the growth reactions need not be similar. This means that the assembly and disassembly processes occur via two steps, with one being the rate-limiting reaction. The following example assumes that the nucleation reaction is the rate-limiting step since that turns out to be the case in one of the experiments on a chromonic liquid crystal. Figure 11 shows the time evolution of the fraction of molecules in assemblies of size $N$ or larger, namely $\alpha_N = 1 - \alpha_1$, due to a 10:1 dilution. Since the growth reactions are fast, the initial, rapid drop in the fraction of molecules in assemblies is due to the fast buildup of assemblies of size $N$, thus "speeding up" the normally slow reverse nucleation reaction. Once this buildup is over, all that is left is the slow breakup of the remaining assemblies of size $N$.

## 5. Computational investigations of the assembly process

There is a rich history of computational calculations involving the spontaneous assembly of molecules. Some of it is detailed in review articles that are referenced earlier.[11,12,17,26,27,29] Since an exhaustive discussion is beyond the scope of this review, examples are chosen from computations that are formulated with chromonic liquid crystals in mind. These usually discuss both the assembly process and the formation of liquid crystal phases, although only the former is included in what follows.

### 5.1. *Non-atomistic models*

One of the first theoretical attempts to include a description of both the assembly process and the liquid-crystalline ordering properties is the work of Taylor and Herzfeld.[33–35] They introduce a single temperature-dependent parameter as the average free energy of association per monomer for each local assembly geometry (spherical, cylindrical,

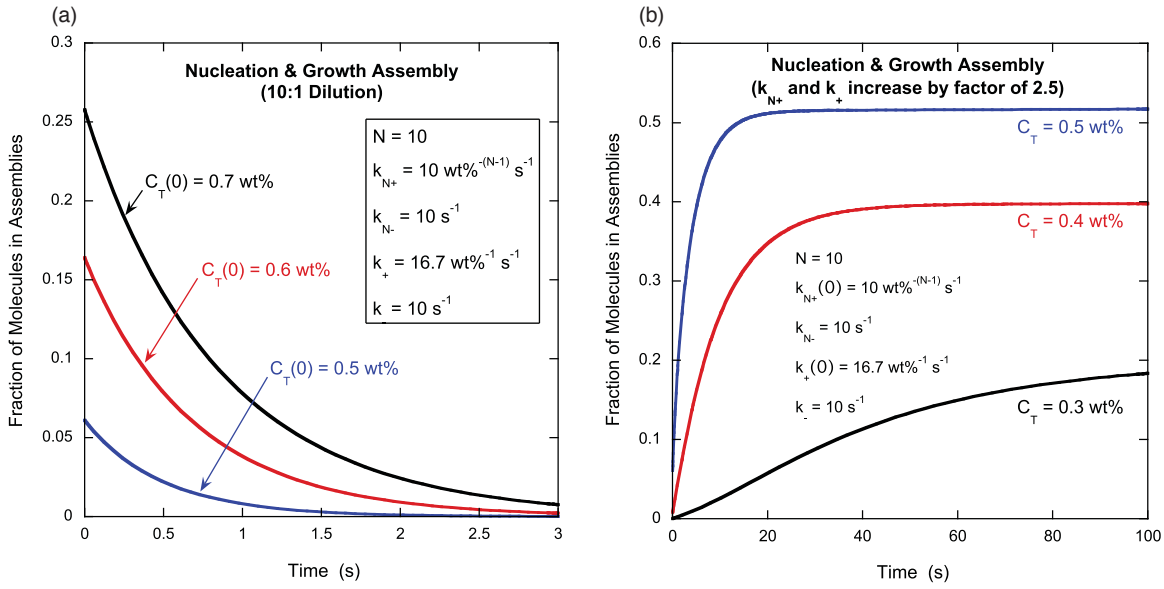


Figure 10. Kinetics of the nucleation and growth model. (a) Results of a 10:1 dilution of systems with varying initial total concentrations in equilibrium with different fractions of molecules in assemblies. (b) The results of increasing both $k_{N+}$ and $k_+$ by a factor of 2.5 for various total concentrations initially at equilibrium with very few molecules in assemblies.

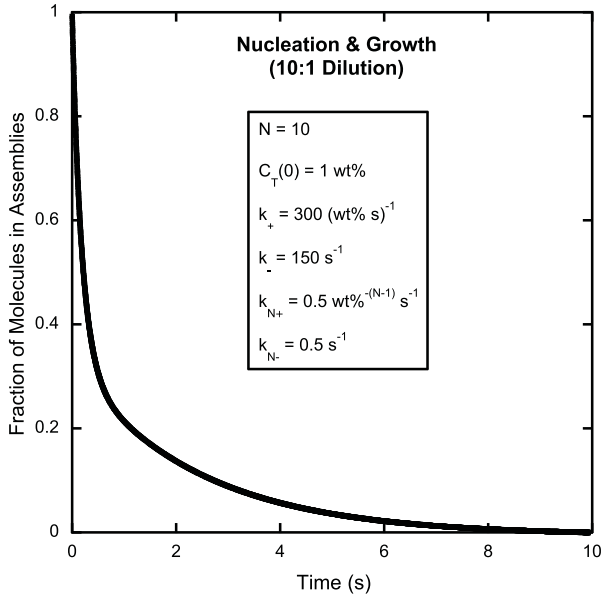


Figure 11. Results of a 10:1 dilution for the nucleation and growth model in which the breakup of the nucleus is the rate-limiting step. The assemblies quickly break up into assemblies close to the size of the nucleus and then more slowly the remaining nuclei break up.

and planar). The system free energy has terms representing ideal mixing, association, and inter-assembly interactions. In the case of rod-like assemblies and no inter-assembly interactions, this results in the same predictions as the isodesmic model based on chemical reactions. That is, if $-\Delta f k_B T$ is the association free energy change per monomer, then the equilibrium constant times the total concentration $KC_T$ in the chemical reaction isodesmic model is equal to $\phi\, e^{\Delta f}$, where $\phi$ is the volume fraction (volume of all of the molecules divided by the volume of the solution).[1] So for example, the average assembly size $\langle i \rangle$ can be written in two ways.

$$\langle i \rangle = \tfrac{1}{2}(1 + \sqrt{1 + 4\,KC_T}) = \tfrac{1}{2}(1 + \sqrt{1 + 4\phi\, e^{\Delta f}}). \quad (21)$$

If $KC_T = \phi\, e^{\Delta f} >> 1$, then Equation (21) reduces to the well-known result $\langle i \rangle \approx \sqrt{KC_T} = \sqrt{\phi\, e^{\Delta f}}$.[36]

Also considered is the case of cylindrical assemblies with spherical end caps. It is assumed that $N$ molecules are needed to form two end caps, meaning there are no assemblies made up of less than $N$ molecules. Molecules can be added to the cylindrical part of the assemblies one-by-one, meaning that each assembly is made up of $N$ molecules in the end caps and any number of molecules in the cylindrical portion. If free energies of association are defined by $-\Delta f_0 k_B T$ and $-\Delta f_1 k_B T$ for the spherical and cylindrical regions, respectively, the calculation follows the nucleation and growth assembly model discussed previously. For example, for the nucleation and growth model when $\sigma$ and $N$ are large, the concentration for the onset of assembly formation (the critical micelle concentration) is approximately given by $1/(\sqrt[N-1]{\sigma}K) = 1/\sqrt[N-1]{K_N} = 1/K_E$, which translates to another well-known relation, namely that the critical volume fraction in this case is approximately $e^{-\Delta f_0}$.

A quite different method utilizes a Monte Carlo simulation of a mixture of chromonic disks and solvent spheres.[37] The chromonic disks are made from seven hard spheres of the same diameter bonded together in a plane. The center sphere is solvent-phobic with a hard-core exclusion distance of twice its diameter, but has an attractive disk–disk square-well potential extending out to

twice its diameter. The six outer spheres interact with the solvent spheres just as the solvent spheres interact with each other, namely through a square-well potential with a hard core equal to the sphere diameter and an attractive region extending out to three-halves of a sphere diameter. Parameters for the simulations are set for the purpose of investigating the formation of both linear assemblies and lyotropic liquid crystal phases.

Although the results of the simulation follow the isodesmic assembly model, one of the most interesting findings stems from using the simulation to determine the average equilibrium constant for adding a disk to assemblies of various sizes (still in the isotropic phase). The expectation is that the equilibrium constant should depend on temperature according to Equation (17) and not be concentration dependent. This is borne out by the simulation, but only at intermediate volume fractions ($0.3 < \phi < 0.6$). For lower and higher volume fractions, especially at low temperatures, the equilibrium constant does not follow Equation (17) and varies with concentration. The conclusion is that at high enough temperatures, this model system acts as one would expect from an isodesmic assembly model. But such is not the case for lower temperatures and the reason may be associated with the nearness of the limit of complete assembly in which the distribution of assembly sizes is flat.

A continuation of this work is a Monte Carlo simulation that utilizes a nine hard sphere, bonded diamond-shaped structure along with the seven-hard sphere disk structure just discussed.[38] The six outer spheres of the seven sphere disk-shaped structure are hydrophilic and the central sphere is hydrophobic. For the nine sphere diamond-shaped structure, the seven spheres that form a disk are hydrophobic and the two spheres on opposite sides of this disk are hydrophilic. The attractive interaction among hydrophilic spheres and spheres representing water are modeled with a Lennard–Jones potential. Hydrophobic–hydrophilic interactions are modeled by a truncated and shifted Lennard–Jones potential. The simulations reveal the formation of assemblies for the diamond-shaped structures but not for the disk-shaped ones. Two results from the simulations with the diamond-shaped structures have direct bearing on how well this simulated system follows the isodesmic assembly model. First, a plot of the average size versus volume fraction follows a power law with an exponent of around 0.6 for average sizes below 10, but the exponent seems to increase significantly when the assemblies are larger than this. Equation (21) predicts that for average assembly sizes less than 10, the exponent should be slightly less than 0.5, with the exponent approaching 0.5 for larger average sizes. Second, the free energy between a disk and a single disk, two disks, and three disks varies somewhat. Both of these findings question whether the assumption of isodesmic assembly is always an appropriate one.

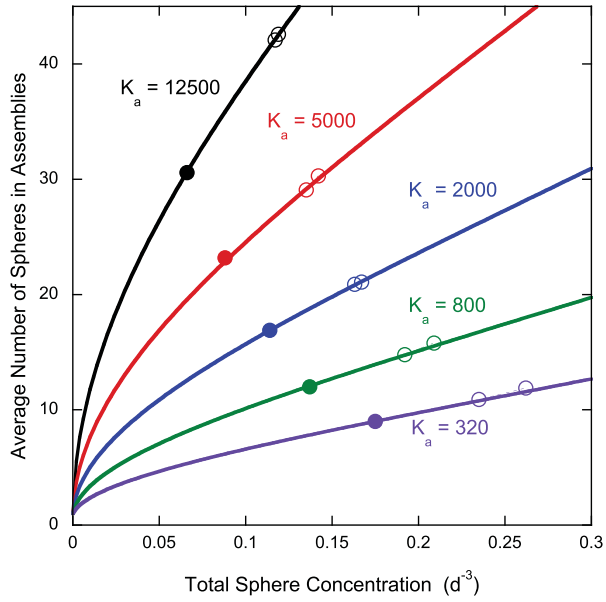


Figure 12. Comparison of the theoretical prediction and simulation results in the isotropic phase according to of Ref. [39, Table I] Five association constants $K_a$ and two persistence lengths $\ell_p(100d$ for open circles and $1000d$ for filled circles) are shown. The curves use a modified version of Equation (21), namely with the total concentration $\rho$ taking the place of $\phi$, $\Delta f$ given as $\ln K_a$, and $\kappa\rho$ added to $\Delta f$ ($\kappa = 1.45\ d^3$).

In a slightly different simulation, the Monte Carlo method is used for hard spheres which can bond together with a bond energy (in units of $k_BT$) specified as $\ln(K_a)$, where $K_a$ is the association constant, independent of assembly size.[39] In addition, the bending potential for the angle between any three consecutive bound spheres is an infinite square well between $\theta_{\min}$ and $\theta_{\max}$ and no junctions or branch points are permitted. The values of $\theta_{\min}$ and $\theta_{\max}$ determine the persistence length of the assembly $\ell_p$, given in units of an hypothetical distance $d$. The average assembly size varies with total sphere concentration as predicted by Equation (21), at least at low sphere concentration. The simulation results at higher sphere concentration correspond to an isodesmic assembly model that takes into account end effects, since the excluded volume of a sphere at the end of the assembly is greater than that for an interior sphere. This amounts to adding a term $\kappa\phi$ to $\Delta f$ in Equation (21). As can be seen from Figure 12, this produces excellent agreement with the simulation results. Notice also that assembly size does not depend on $\ell_p$, because assembly is governed by $K_a$ alone. The distribution of assembly sizes in the isotropic phase is a decreasing exponential function of assembly size as in the isodesmic assembly model, but this breaks down in the nematic phase where the data approximate a sum of two exponential functions.

In another simulation, hard cylinders of length $L$ and diameter $D$ experience short-range attractive interactions

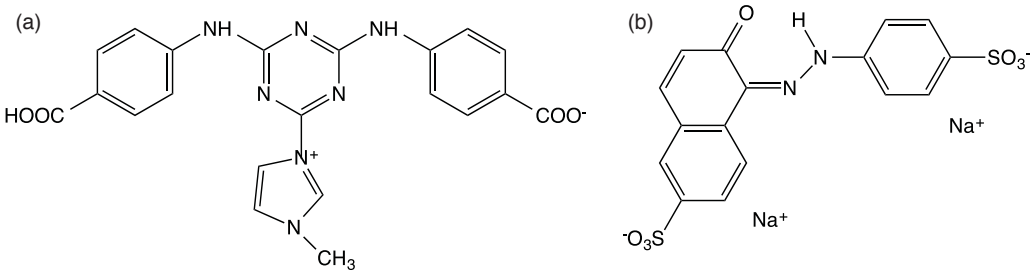


Figure 13. Molecular structure of (a) NMI and (b) Sunset Yellow FCF.

between cylinder ends.[40] The shape of the attractive potential is tuned slightly to promote the formation of linear as opposed to branched assemblies. Aspect ratios $L/D$ of 0.5, 1, and 2, along with binding energies ranging from 0 to 12 $k_BT$ are examined. The average number of cylinders in assemblies grows slowly with volume fraction in the isotropic phase, after which it increases much more rapidly with volume fraction in the nematic phase. In the isotropic phase, the concentration of different assembly sizes decreases exponentially with increasing size up to a size of about 60, in accordance with the isodesmic assembly model.

### *5.2. Atomistic models*

Recently, researchers have been able to simulate the behavior of large numbers of actual chromonic liquid crystal-forming molecules in solution. One of the first molecules investigated in this way was 3-[6-(3-carboxyanilino)-4-(3-methyl-1H-imidazol-s-ium-1-yl)-1,3,5-triazin-1-ium-2-yl] aminobenzoate (NMI).[41] The structure of the NMI molecule is shown in Figure 13(a). A semi-empirical quantum mechanics code is used to determine the conformation and electronic structure of NMI in water. Then, a molecular dynamics algorithm is utilized to follow the behavior of multiple molecules in water. Starting with a random distribution of molecules, stacks of molecules form during the simulation. The calculated X-ray diffraction pattern using the results of the molecular dynamics simulation displays a peak corresponding to a stacking distance of 0.33 nm. The stacks are not always of single molecules; often stacks of three- and four-member rings are observed. The calculated stacking free energy changes per molecule are about 2 $k_BT$ for single stacks and approximately 6 $k_BT$ for four-member rings, with roughly 40% of the free energy change due to the $\pi - \pi$ interactions between neighboring molecules in a stack.

A more detailed simulation concerns the disodium salt of 6-hydroxy-5-[(4-sulfophenul)azo]-2-naphthalene sulfonic acid or Sunset Yellow FCF (SSY) shown in Figure 13(b).[42] Quantum chemical calculations using density functional theory determine the structure of the molecule. Molecular dynamics then simulates the dynamics of SSY for both dilute and concentrated solutions. Starting from a random arrangement of 8 molecules, less than 1 ns of simulation time is sufficient to see initial formation of dimers in solutions. Two tetramers appear after about 20 ns and a single stack of 8 molecules is present after 200 ns. Two views of the stack of 8 molecules are given in Figure 14. The stacking distance fluctuates, especially around rearrangement locations, but is about 0.34 nm away from these locations. The average distance between the stacks in the nematic phase is approximately 2.3 nm. The free energy of binding can be computed by calculating the work done in "pulling" a molecule from a stack. The results indicate a nearly isodesmic process, with the free energy of binding being 7.4, 6.5, and 6.5 $k_BT$ for removing a molecule from a dimer, trimer, and stack of 8 molecules, respectively.

More recent work addresses assembly in a non-ionic system, namely 2,3,6,7,10,11-hexa-(1,4,7-trioxa-octyl)-triphenylene (TP6EO2M), the molecular structure of which is in Figure 15.[43] Again molecular calculations are first carried out, followed by molecular dynamics simulations of a collection of molecules in water. Two force fields are used; one produces results differing significantly from experimental observations but the other results in simulations in accord with experiment. Assembly occurs quickly in the simulations, with dimers and trimers showing up within 10 ns, 2 stacks of 2 and 6 molecules appearing within 50 ns, and a stack of 8 molecules resulting after 90 ns. Two stacking distances are examined in the stack of 8 molecules: an inter-molecular distance between the center of mass of 2 neighboring molecules and an inter-layer distance defined perpendicularly from the molecular planes of 2 neighboring molecules. The former distance averages about 0.46 nm and the latter distance is 0.37 nm on average. This difference indicates that the molecules are offset from one another in the stack. The free energies of association are a bit larger for these molecules, 17.5, 14.5, and 14.4 $k_BT$ for binding a molecule to another molecule, a dimer, and a trimer, respectively. Again, the quasi-isodesmic character of the assembly process is revealed by the slightly larger free energy for dimer formation over the addition of a molecule to a stack of molecules

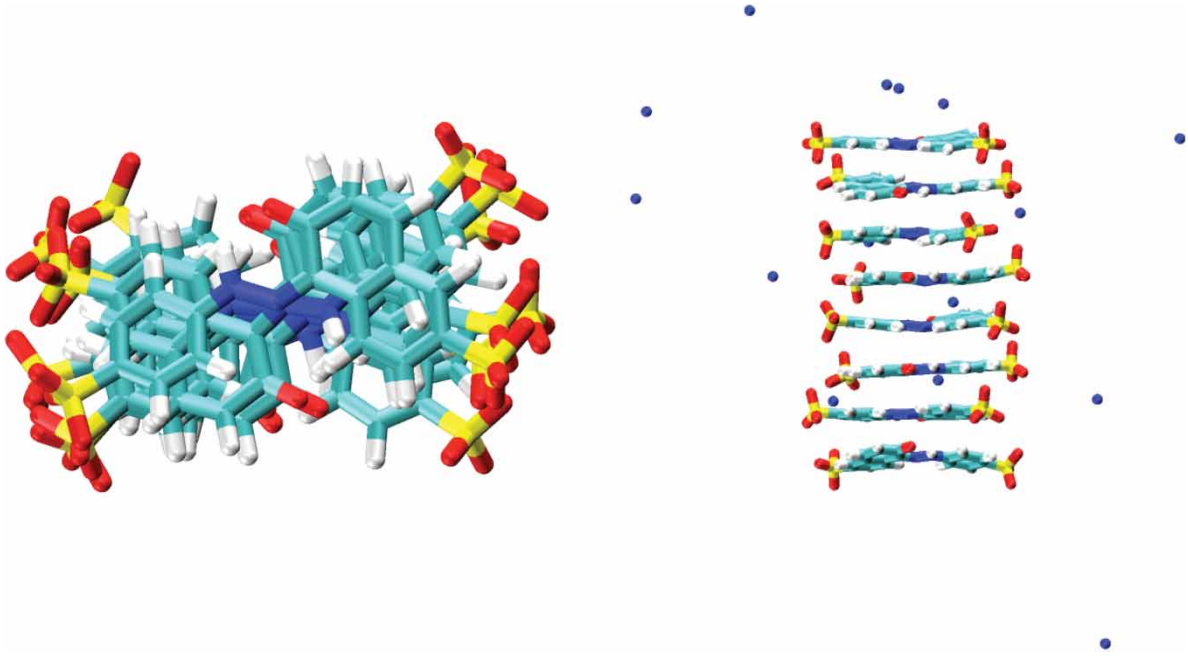

Figure 14. Snapshots of the stack of 8 SSY molecules. The left-hand view is down the stack and the right-hand view is from the side of the stack. Notice the alternation of the orientation of the molecules in the stack. Reprinted with permission from *Journal of the American Chemical Society*. Copyright 2010 American Chemical Society.[42]

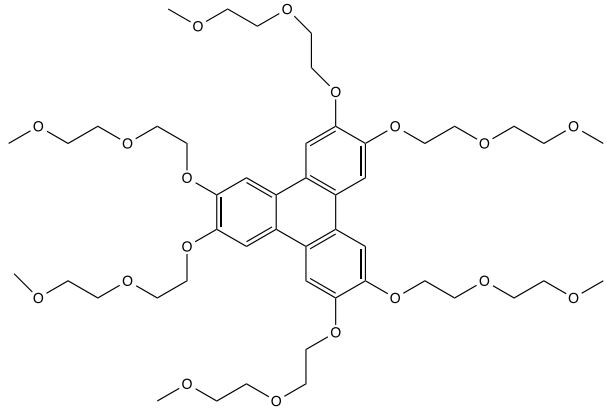

Figure 15. Molecular structure of TP6EO2M.

(see Figure 16). The simulation also demonstrates that the average number of water molecules around the oxygen atoms in the chains decreases when a single molecule joins a stack of molecules.

A thermodynamic analysis is also useful in the simulations. Determining the free energy of association of a molecule to a stack of three molecules for different temperatures allows the free energy to be decomposed into enthalpy and entropy contributions. Over a temperature range of 280–320 K, the enthalpy is relatively constant at roughly $-12\ k_BT$ while the temperature times the entropy increases from around 16 $k_BT$ to about 19 $k_BT$. In general, although both contributions favor forming assemblies, the entropy contribution is greater than the enthalpy contribution.

Atomistic simulations are extremely intensive computationally, encouraging efforts to find faster methods. One such "course graining" technique also deals with the assembly of TP6EO2M. Instead of starting with the actual molecule, a simpler structure for a dissipative particle dynamics simulation is employed.[44] The triphenylene core is represented by a hexagon with 12 particles on its perimeter and 7 internal particles. Each ethylene oxide chain is represented by 3 particles. The particles making up the core are different from the particles in the chains. The dissipative particle dynamics parameters are chosen to encourage micro phase segregation, allowing the ethylene oxide arms and water to freely mix, but keeping the triphenylene core separate. The reduced number of particles allows the simulated system to contain many more "molecules". One result of the simulation is that the preference for dimers over monomers is greater than expected for an isodesmic assembly process. This preference is quantified by constructing Van't Hoff plots of ln $K$ versus $1/T$, from which it is found that the association enthalpy for dimer formation and assembly growth are very similar at $-15.2\ k_BT$, but the entropy for dimer formation and assembly growth are $-9.0\ k_B$ and $-10.6\ k_B$, respectively. While these values differ from the atomistic simulations, it is noted that the parameters of the dissipative particle dynamics simulation can be tuned to give the association enthalpy that results from atomistic simulations in dilute solutions.

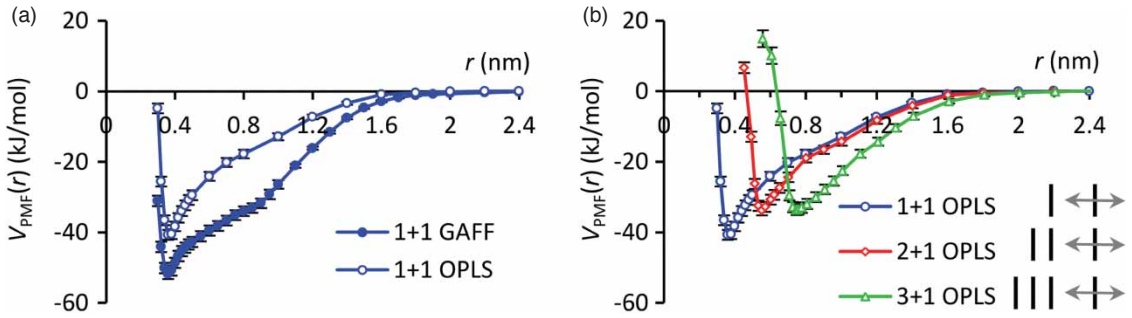


Figure 16. Free energy of association for two force fields, general Amber force field and optimized potentials for liquid simulations (OPLS). (A) Free energies as a function of separation for two single molecules using the two force fields. (B) Free energy as a function of separation for two single molecules, for a dimer and a single molecule, and for a trimer and single molecule using the OPLS force field. Reproduced from Ref. [43] with permission from The Royal Society of Chemistry.



## 6. Experimental investigations of the assembly process

The main experimental techniques that are used to study chromonic liquid crystals are X-ray diffraction and optical investigations such as polarized optical microscopy and optical spectroscopy. Also of use are nuclear magnetic resonance (NMR) experiments and light scattering investigations. Some of these experiments reveal information on the assembly process, and it is these that are addressed in what follows. It is beyond the scope of this review to include all of the work; recent reviews, however, provide a much more comprehensive summary.[11–17]

### *6.1. X-ray measurements*

X-ray diffraction provides critical information on the assembly process in chromonic liquid crystals. The first report on DSCG (see Figure 17(a) for its chemical structure) includes X-ray measurements done in two liquid crystal phases.[5] Two results from this and later work point to a rod-like assembly structure made from stacks of molecules. The first piece of evidence is a reflection indicating a repeat distance of 0.34 nm that is independent of concentration and temperature. This distance is typical of the separation between aromatic structures, including the atomic planes in graphite and the separation of base pairs in DNA. The conclusion is therefore that the assemblies involve molecular stacking. The second result is the observation of a reflection that represents a much larger distance and varies with concentration. This is noteworthy due to some very simple geometrical ideas on how structures of different shape respond to changes in concentration. The best way to see this connection is to consider volume fraction $\phi$ instead of concentration. If the assemblies are very large parallel sheets of thickness $a$ and separation $d$, then $\phi$ is simply $a/d$. If the assemblies are very long parallel rods with a square cross-section of side $a$ and separated by $d$ on a square lattice, then $\phi$ equals $(a/d)^2$. Finally, if the assemblies are cubes of side $a$ separated by $d$ in a cubic lattice, then $\phi$ equals $(a/d)^3$. Considering circles instead of squares and spheres instead of cubes introduces a constant in the equation for $\phi$, but the dependence on $a/d$ remains the same. So if an X-ray experiment measuring $d$ is performed at different volume fractions, how $d$ depends on $\phi$ points to a particular shape for the assemblies. Many of the results of such X-ray experiments have been collected in recent articles, where the dependence of $d$ on $\phi$ is consistent or very nearly consistent with an exponent of $\frac{1}{2}$, as expected for long rods.[45,46] Thus, models for linear assemblies are the ones appropriate for these systems.

The results of a much more recent X-ray experiment on DSCG are shown in Figure 18.[47] The refections from both the molecular stacking distance (0.34 nm) and the inter-assembly distance (4.5 nm) are clearly shown, along with some concentration-independent reflections probably associated with the molecular structure of DSCG. The chromonic liquid crystal is oriented by a magnetic field, showing that the direction of stacking is perpendicular to the inter-assembly distance. This is consistent with a stack of molecular planes perpendicular to the long axis of the linear assemblies.

X-ray experiments can be done with the goal of investigating the length of the assemblies. The correlation length corresponding to the stacking of the molecules can be determined from the half-width of the X-ray reflection due to molecular stacking.[48] If this correlation length is taken to be the length of the assembly, then the free energy change due to stacking can be determined if the volume fraction is known. For the chromonic liquid crystal Sunset Yellow FCF, a value of about 5.7 $k_BT$ is found. The importance of recognizing that most molecules that form chromonic liquid crystals are charged, should be taken into account. The most simple way to do this is to realize that the free energy change measured in an experiment may be lower by about 2 $k_BT$ from the uncharged case due to this repulsive interaction. In later work, the temperature dependence of the correlation length for SSY is used and a value of $(4.3 \pm 0.3)$ $k_BT$ is obtained.[49] This work also reveals that the free energy change is slightly concentration

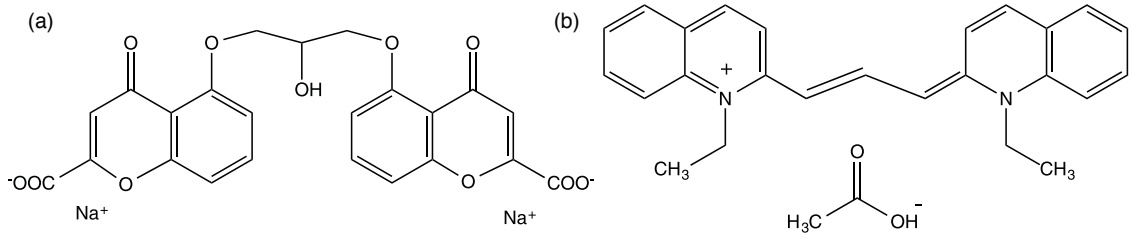


Figure 17. Molecular structures of (a) DSCG and (b) pinacyanol acetate.

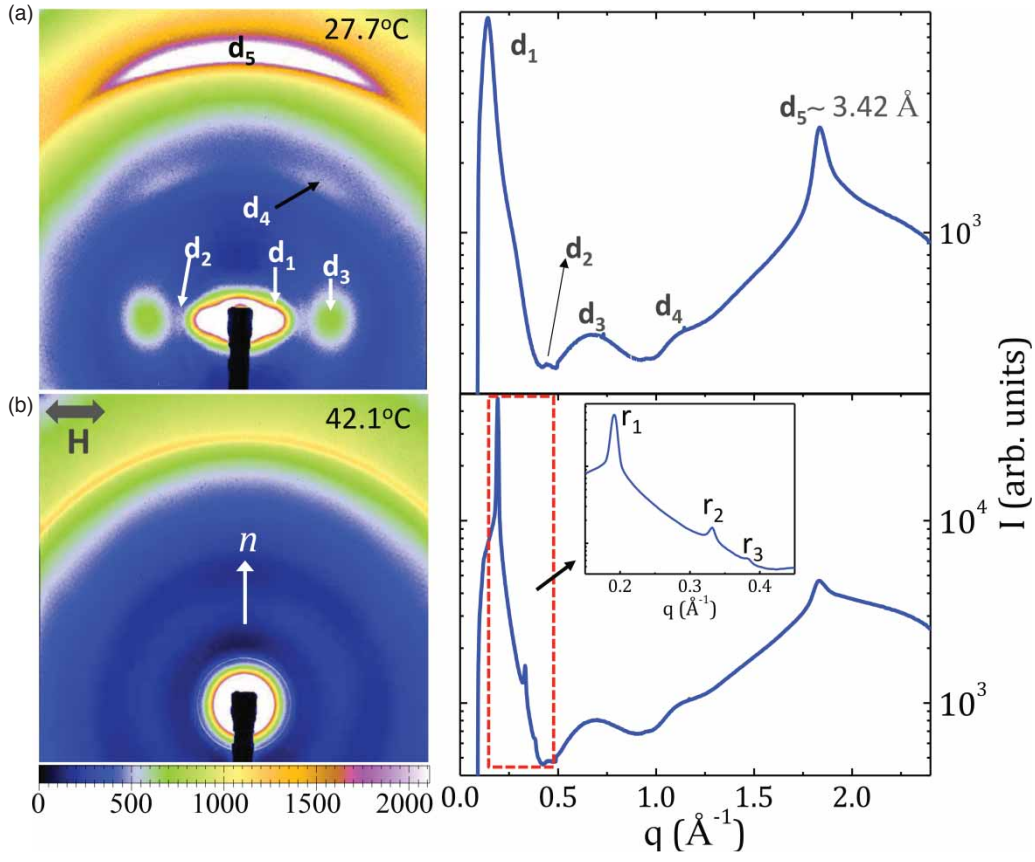


Figure 18. X-ray diffraction of the nematic phase (a) and the columnar–isotropic biphasic region (b) of a 15 wt% sample of DSCG. The reflection from the stacking separation is denoted $d_5$ and the reflection from the inter-assembly distance is labeled $d_1$ (in (a) equal to 44.5Å). The right-hand figure is the integrated intensity profile of the left-hand figure. The reflections shown in the inset of (b) are from lengths $r_1 = 32.8$Å, $r_2 = 18.9$Å, and $r_3 = 16.4$Å, corresponding to the $1 : \sqrt{3} : 2$ ratios expected for the hexagonal packing of the columnar phase. Reproduced from Ref. [47] with permission from the American Physical Society.

dependent. These results indicate that the assumption of isodesmic assembly is warranted, but it should be viewed as a first step and not exact.

X-ray measurements also show that the assemblies in some liquid crystals are more complicated than a stack of molecules or even a stack of molecules with a cross-section of two or more molecules. For the chromonic liquid crystal pinacyanol acetate, shown in Figure 17(b), the inter-assembly distance is as large as 20 nm in the liquid crystal phase, significantly larger than found in such systems as DSCG and SSY.[22] In addition, the concentration of pinacyanol acetate is much lower. Since the dependence of the inter-assembly distance still depends on the volume fraction to the half power, the assembly must elongate in one dimension. These data along with additional data from a point-collimated small angle X-ray diffraction experiment are consistent with a hollow cylinder structure, in which the pinacyanol acetate molecules are in a thin shell around the outside of an inner core of water. The diameter of the assembly is about 4.6 nm, much more than a molecular

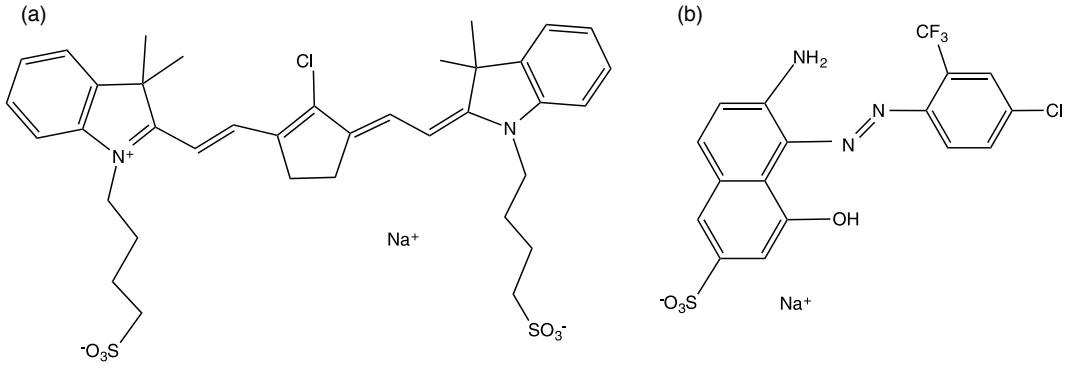


Figure 19. Molecular structure of (a) IR-806 and (b) Acid Red 266.

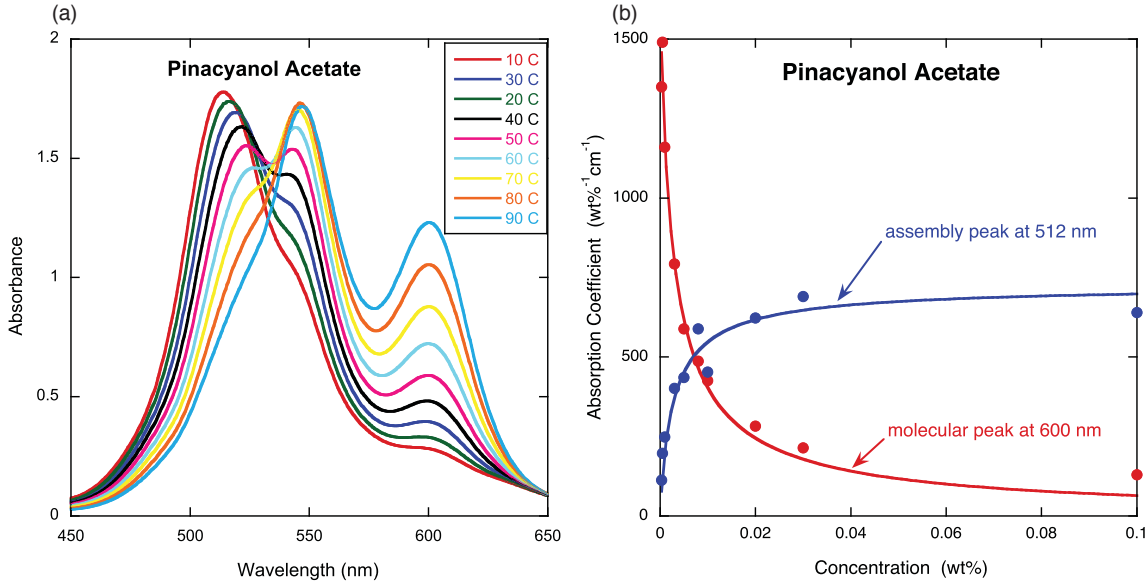


Figure 20. Variation of the peaks due to single molecules and molecules in assemblies with temperature and concentration for pinacyanol acetate (from Ref. [50]). (a) The concentration is fixed at 0.0075 wt% in a 1 mm cell and the temperature is varied. The spectra can be decomposed into six Gaussian peaks with constant center wavelengths and widths but changing magnitude as the concentration or temperature is changed. (b) The result of the decomposition for room temperature spectra of different concentrations with plots of the magnitude of two peaks, one representing single molecules and one representing molecules in assemblies. These peak magnitude data are fit to the isodesmic assembly model simultaneously, yielding a value for the stacking free energy of 10.3 $k_BT$.

dimension. A similar case is the chromonic liquid crystal IR-806 (chemical structure shown in Figure 19(a)), in which X-ray diffraction measurements indicate that the inter-assembly distance is about 15 nm.[23]

### *6.2. Absorption measurements*

For many chromonic liquid crystal systems, the absorption coefficient spectrum depends on the distribution of assembly sizes. In some cases, the change is not dramatic. In other cases, the absorption coefficient spectrum possesses multiple peaks that increase and decrease during the assembly process. In the former case, theories for both the assembly process and how the absorption coefficient spectrum depends on assembly size must be combined to interpret the data. This can be done for a number of chromonic liquid crystals using the isodesmic assembly model and the exciton model for the electronic structure, yielding values for the stacking free energy change in the 7–12 $k_BT$ range.[21,45] In the latter case, a peak in the absorption coefficient spectrum can often be assigned to either single molecules or molecules in assemblies. Thus, the magnitude of these peaks can be used to track the fraction of single molecules and the fraction of molecules in assemblies. An example of such a measurement is shown in Figure 20 for pinacyanol acetate.[50] The absorption measurements can be taken at constant temperature or constant concentration. The latter are usually more consistent with each other, so the absorption coefficient spectra at a very low concentration and varying temperature for pinacyanol acetate are shown in Figure 20(a). All of the spectra, even spectra at higher concentrations, can be decomposed into six

Gaussian peaks. The center wavelength and full-width at half-maximum (FWHM) of each peak do not change with concentration; only the magnitude of the peak changes. Shown in Figure 20(b) is how the peak at 600 nm due to single molecules and the peak at 512 nm due to molecules in assemblies change with concentration at room temperature, along with a fit to the isodesmic assembly model, Equation (4), for both single molecules and molecules in assemblies simultaneously. The best fit value for $K$ is 204 wt%$^{-1}$, which can be converted to a stacking free energy change through $KC_T = \phi\, e^{\Delta f}$, because $\phi$ is proportional to $C_T$ at these low concentrations. The result is a stacking free energy change of 10.3 $k_BT$. Similar measurements on IR-806 yield a stacking free energy change of 9.0 $k_BT$.[23] It is interesting to check whether these data are consistent with a simple dimerization reaction instead of isodesmic assembly. When the data of Figure 20(b) are fit to a reaction in which two molecules form a dimer, the fit is not as good, with a $\chi^2$ value 32% higher. When the same check is applied to the IR-806 data, the $\chi^2$ value increases by a factor of over 4 for the fit to dimerization.[23]

An example that in some ways falls between the two cases outlined above are the UV/VIS measurements on Acid Red 266 (see Figure 19(b)).[51] Although there is little structure in the absorption spectrum, the spectrum can be decomposed into the split bands due to assembly. Although it is not possible to distinguish dimerization from isodesmic assembly, the enthalpy driving the reaction is found to be $(-8.9 \pm 0.2)\ k_BT$ with a positive entropy times temperature of about 0.8 $k_BT$. From determinations of the single molecule concentration as a function of total concentration, a stacking free energy change of about 12 $k_BT$ can be calculated.[45]

Absorption measurements have also been done in the isotropic phase near the transition to the liquid crystal phase to see if the assembly process continues to be continuous at higher concentrations. These experiments involve measurements of the absorption coefficient at one wavelength as the temperature is varied. The absorption coefficient varies linearly over a wide range of temperature in SSY, but in DSCG there is a sharp change in slope roughly 10 K above the nematic–isotropic coexistence region.[46]

There seem to be two classes of chromonic liquid crystals. One forms a liquid crystal phase at room temperature for concentrations somewhere in the vicinity of 10 wt% (the range is actually quite wide, from less than 10 wt% to over 30 wt%). The other class forms a liquid crystal phase at room temperature for much lower concentrations, typically less than 1 wt%. When the assembly process is probed at extremely low concentrations, both classes more or less act the same, with something close to isodesmic assembly and a stacking free energy in the 10 $k_BT$ range. Actually, the systems that form a liquid crystal phase at the low concentrations tend to have a higher stacking free energy change. Whereas this nearly isodesmic assembly process seems to continue right to the formation of the liquid crystal phase for the first class of materials, such is not the case for the second class. For at least some of the compounds that form a liquid crystal phase at concentrations below 1 wt%, there is a second step in the assembly process at higher concentration but before the liquid crystal phase forms. Initial investigations of this second step are producing evidence that it is not continuous, but closer to a process with a sharp threshold.

The system from this second class that has received the most attention is IR-806. In order to perform a thorough thermodynamic analysis, measurements are taken with both concentration and temperature being varied.[52] Varying the temperature at constant concentration turns out to be a much more precise technique, since precise control of the concentration is more difficult than controlling the temperature. For IR-806, this second step occurs over about a 25°C range that varies with concentration. As can been seen from Figure 21, for a 0.4 wt% sample the range is from 10°C to 35°C.[53] At temperatures above this range, the spectrum is dominated by a peak at 660 nm. At temperatures below this range, a peak at 830 nm dominates the spectrum. Notice the well-defined isosbestic point at 723 nm, indicating that there are only two absorbing species involved. One must be the intermediate assemblies that result from the quasi-isodesmic assembly process and the other must be the large assemblies that form as a result of this second step in the overall assembly process. By performing similar experiments at concentrations below and above 0.4 wt%, pairs of points in the temperature–concentration plane with the same absorption coefficient spectrum can be identified. If these

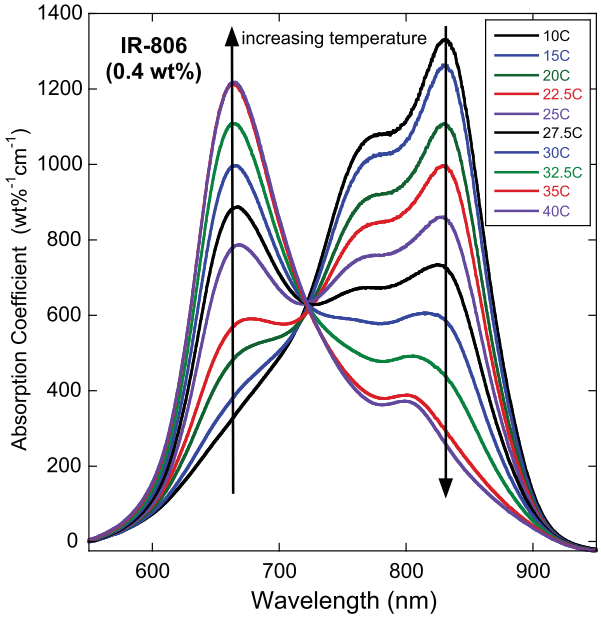


Figure 21. Absorption coefficient spectrum of a 0.4 wt% sample of IR-806 at different temperatures (from Ref. [53]).

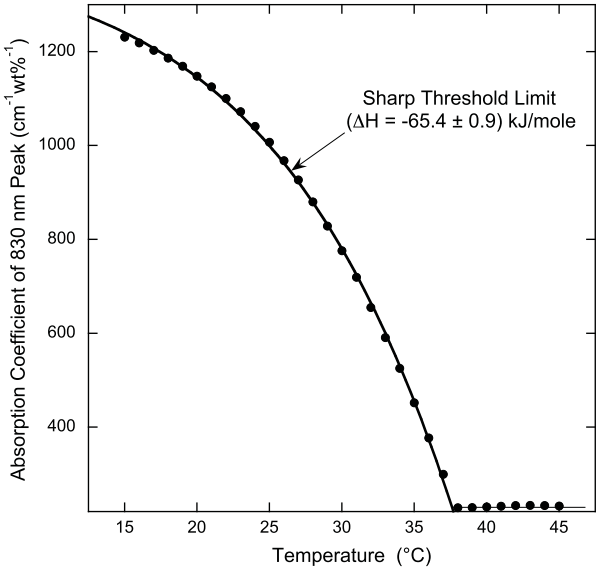


Figure 22. Absorption coefficient of the 830 nm peak versus temperature for a 0.3 wt% solution of IR-806. The solid line is the theoretical prediction for the limit of a sharp threshold, Equation (18), and yields a value for the enthalpy during growth of $(-65.4 \pm 0.9)$ kJ/mol. Reprinted with permission from *Journal of Physical Chemistry B*. Copyright 2014 American Chemical Society.[52]

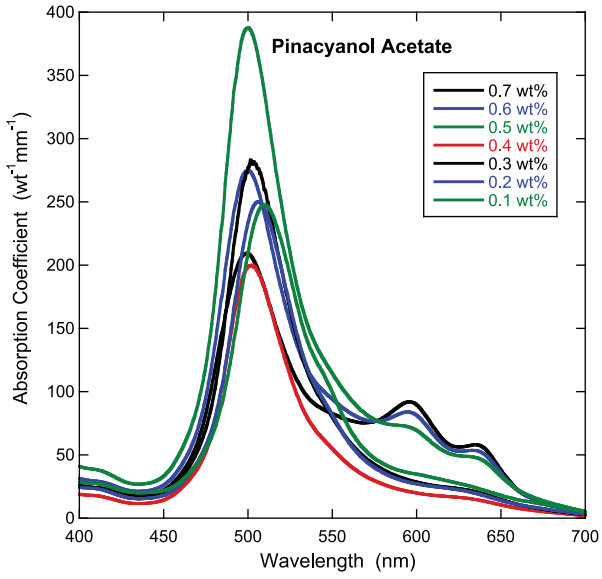


Figure 23. Absorption coefficient of pinacyanol acetate solutions at various concentrations (from Ref. [54]). The second step of the assembly process is evident when the two peaks around 600 and 640 nm appear.

are assumed to represent the same assembly condition, a modified form of the van't Hoff equation can be used to estimate the enthalpy of this reaction, which turns out to be − 50 kJ/mol.[52]

A more precise analysis can be performed by decomposing the absorption coefficient spectra at a fixed concentration and determine the magnitude of the 830 peak (representing the large assemblies) as a function of temperature. If the magnitude of this peak is assumed to be proportional to the number of intermediate assemblies in the large assembly, then it can be compared to theoretical predictions. As shown in Figure 22, the data are consistent with the theory in the sharp threshold limit, Equation (18), and yield a value for the enthalpy of $(-65.4 \pm 0.9)$ kJ/mol. In short, the second step of the assembly process in IR-806 is very different from the first step; the former has a sharp threshold while the latter is continuous.

A two-step assembly process is also present in pinacyanol acetate. As assembly takes place at the lowest concentrations, a peak in the absorption coefficient spectrum around 600 nm gives way to a peak around 520 nm in a process that appears to be isodesmic (see Figure 20(a)). But at higher concentrations starting around 0.5 wt%, two peaks in the vicinity of 620 nm begin to grow at the expense of the 520 nm peak.[54] This is shown in Figure 23. As will be explained later in the section on kinetics, there is evidence that this step also has a sharp threshold.

This is not the first time a two-step process is observed in a system in which self-assembly occurs. For example, oligo(*p*-phenylenevinylene) derivatives with chiral side chains form disordered stacks via an isodesmic assembly process at high temperatures, but upon lowering the temperature nucleation of ordered chiral stacks occurs with a sharp threshold, followed by elongation of the assemblies. Measurements of the circular dichroism reveal data that closely resemble the absorption data in Figure 22.[55]

### 6.3. *Light scattering measurements*

Light scattering experiments are useful in probing assembly processes because they are sensitive to the concentration, size, and shape of the assemblies. For example, while the change in the absorption coefficient spectrum might be attributable to either isodesmic assembly or dimer formation, light scattering can tell the difference. This is illustrated quite nicely when experiments are done on PIC (shown in Figure 24(a)) at concentrations below and above the concentration at which a sharp, red-shifted absorption band appears. Analysis of the data indicates that just below the appearance of the assembly absorption band, the average number of molecules in an assembly is about 60, and increases to over 1000 as the concentration increases.[56] Likewise, static light scattering measurements on Acid Red 266 at concentrations below 0.05 wt% indicate assemblies with between 200 and 2000 molecules that have a Gaussian coil or worm-like structure.[51]

More recent light scattering investigations of chromonic liquid crystals have concentrated on either the isotropic phase near the nematic–isotropic coexistence region or in the liquid crystal phases themselves. As the coexistence region is approached by decreasing the temperature, there

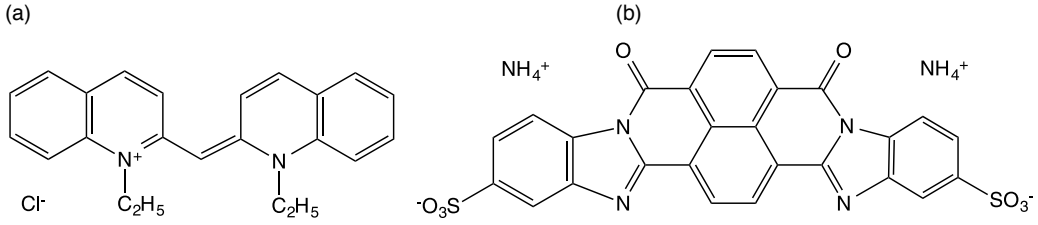


Figure 24. Molecular structure of PIC (a) and Bordeaux dye (b).

is an increase in light scattering for two reasons: (1) the size and concentration of the assemblies is increasing, and (2) pretransitional fluctuations of orientational order are increasing. In an experiment using DSCG, the fact that both of these contribute to light scattering can be verified. In addition, dynamic light scattering results indicate that there are two fluctuating modes: one rapidly slows down as the temperature approaches the coexistence region, but the other remains fairly constant. The first is associated with the relaxation of orientational fluctuations and the second is a diffusion mode of concentration fluctuations.[57] In later work utilizing improved techniques, a change in the assembly process is observed about 12 K above the nematic–isotropic coexistence region. The temperature dependence of the scattering intensity suddenly changes and the intensity autocorrelation function changes shape as shown in Figure 25.[58] These findings are a clear indication that in DSCG, the nature of the assembly process changes as orientational order begins to set in. This feature is not universal, as similar light scattering experiments on the chromonic liquid crystal Bordeaux dye (chemical structure shown in Figure 24(b)) do not show this sudden change.[46]

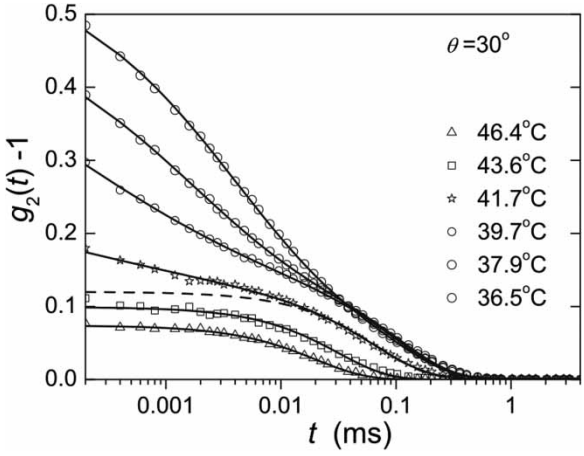


Figure 25. Polarized scattering intensity correlation functions for 10 wt% DSCG (vertical–vertical alignment and a scattering angle of 30°). Notice how the correlation function changes between 43.6 °C and 41.7°C, roughly 10°C above the coexistence region. The solid curves are fits to a single exponential mode below the dashed line and for a combination of single exponential and stretched exponential modes above the dashed curve. The dashed curve is a fit to a single exponential mode for the 41.7°C data. Reproduced from Ref. [58] with permission from the American Physical Society.

### *6.4. NMR measurements*

NMR spectroscopy is a useful tool to probe the assembly process in chromonic liquid crystal systems. When DSCG is dissolved in $D_2O$, for example, the deuteron quadrupole splitting is sensitive to DSCG concentration, temperature, and NaCl concentration.[59] Some of the $D_2O$ molecules are associated with DSCG molecules, and if the DSCG molecules are partially ordered by the magnetic field, then there is a splitting of the deuteron quadrupole resonance. It must be kept in mind that the assemblies align with their axes perpendicular to the magnetic field due to the diamagnetic anisotropy of the individual DSCG molecules. The transition from the isotropic to the nematic phase is quite evident, as is the increase in the nematic order parameter with decreasing temperature and increasing NaCl concentration. Only one splitting is observed, indicating that either there is only one type of water associated with the assemblies (e.g. no inside versus outside water) or that the exchange rate between two such types of associated water is fast enough to average out the difference in splittings.

Na-23 NMR spectroscopy is useful for studying systems that contain sodium atoms or systems without sodium atoms but added NaCl.[60] In the liquid crystal phases, the quadrupole splittings increase as the DSCG concentration increases, but eventually start to decrease at higher DSCG concentrations. The effect of added NaCl is monotonic, with the splitting decreasing as the NaCl concentration increases. This may reflect two solvation sites for the sodium ions, each with a different sign of the quadrupole interaction. More interesting for the assembly process is the observation that the FWHM of the single NMR peak in the isotropic phase suddenly starts to increase with decreasing temperature about 10–15°C above the transition from the isotropic phase to the coexistence (N and I) region. This is interpreted as an abrupt onset of assembly formation (non-isodesmic) and, as has been already noted, is clearly

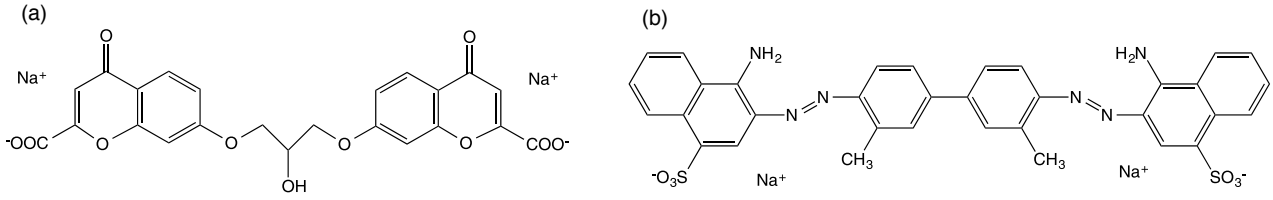


Figure 26. Molecular structure of 7,7′-DSCG (a) and Benzopurpurin 4B (b).



evident in absorption and light scattering measurements on DSCG.

Chromonic liquid crystals with a fluorine atom can be investigated by F-19 NMR spectroscopy.[61] These include some of the azo sulphonic dyes, where a trifluoromethyl group is present. The chemical shift of the fluorine atoms is sensitive to the assembly structure, and in the case of two compounds differing only in the number of sulphate groups, the change of the chemical shift is in opposite directions. As with absorption measurements, it is possible to determine the growth equilibrium constant from the NMR data. Closer examination of the data indicates that for one compound only dimers are formed, but for the other compound larger assemblies are formed. Similar results occur if the compound contains one sulphate group but the trifluoromethyl group is moved to different positions on the aromatic ring. In all cases, the chemical shift decreases with concentration, with some compounds forming only dimers and others forming larger assemblies.[62] Acid Red 266 has a similar structure to these azo sulphonic dyes with a trifluoromethyl group, and F-19 NMR studies reveal a decrease in the chemical shift that is consistent with an isodesmic assembly process. The equilibrium constants determined for Acid Red 266 by NMR and absorption measurements differ by a factor of about 2.5.[51]

NMR can be used to study 7,7′-DSCG, a compound similar to DSCG but with the attachment to each chromone group occurring at the 7 position instead of the 5 position (see Figure 26(a)). As with DSCG, there seems to be an onset of assembly in the isotropic phase 20°C or so above the transition to the nematic phase. What is different from the similar finding with DSCG is that some birefringence is seen with polarizing microscopy between this onset and the nematic phase transition. Deuterium, O-17, and Na-23 NMR are all useful in such studies.[63] NMR relaxation times are also affected by the assembly process. In Benzopurpurin 4B (molecular structure given in Figure 26(b)), the spin-lattice relaxation time increased with temperature smoothly across the transition to the liquid crystal phase. On the other hand, the temperature dependence of the spin–spin relaxation time increases at the point where the liquid crystal phase begins to form.[20]

More recent multinuclear NMR experiments on Sunset Yellow FCF are successful in showing that the hydrazine structure is present in aqueous solution and not the azo structure (the hydrazine structure is shown in Figure 13(b)). In addition, the proton and C-13 chemical shifts decrease with increasing concentration, indicating that the assembly process causes adjacent aromatic groups to shield these nuclei. A stacked structure with the orientation of the molecule alternating along the assembly is proposed.[64] Even more recent work using high resolution proton NMR allowed the chemical shifts of individual protons to be measured.[65] Seven NMR resonances are followed, and all depend on concentration in extremely similar ways. By following these chemical shifts over a large range of SSY concentration, it is shown that the isodesmic model of assembly is too simple to describe the process from very low concentrations where there are mostly single molecules present to concentrations near the nematic phase where mostly assemblies are present. This is demonstrated in Figure 27 for three resonances, where fits to the isodesmic model using all of the concentration data are shown in Figure 27(a), and fits to the four lowest and highest concentration data points are shown in Figure 27(b). It is clear from the figure that the low concentration data are consistent with a much higher equilibrium constant than the high concentration data. The results for the three resonances are consistent, with the low concentration data yielding an average equilibrium constant of $1.78\,\mathrm{wt\%}^{-1}$, and the high concentration data yielding an equilibrium constant of $0.56\,\mathrm{wt\%}^{-1}$. The former indicates a stacking free energy change of 5.5 $k_BT$, which is in good agreement with the X-ray data.[48,49] In addition, these NMR results are consistent with both theoretical and experimental evidence pointing to the fact that the stacking free energy change in SSY decreases as the concentration is increased.[42,49] Analysis of the proton chemical shifts can also be done when adding NaCl to low SSY concentrations. At first, this alters the size and shape of the assemblies but not the fraction of assemblies, whereas at higher NaCl concentrations, the fraction of assemblies increases.[65]

Diffusion NMR measurements are also useful in examining the assembly process. By performing pulsed echo experiments in a magnetic field gradient, the diffusion constant can be determined. The measurements can be compared to predictions for the diffusion of an isodesmic distribution of ellipsoids. When this is done, it points to a

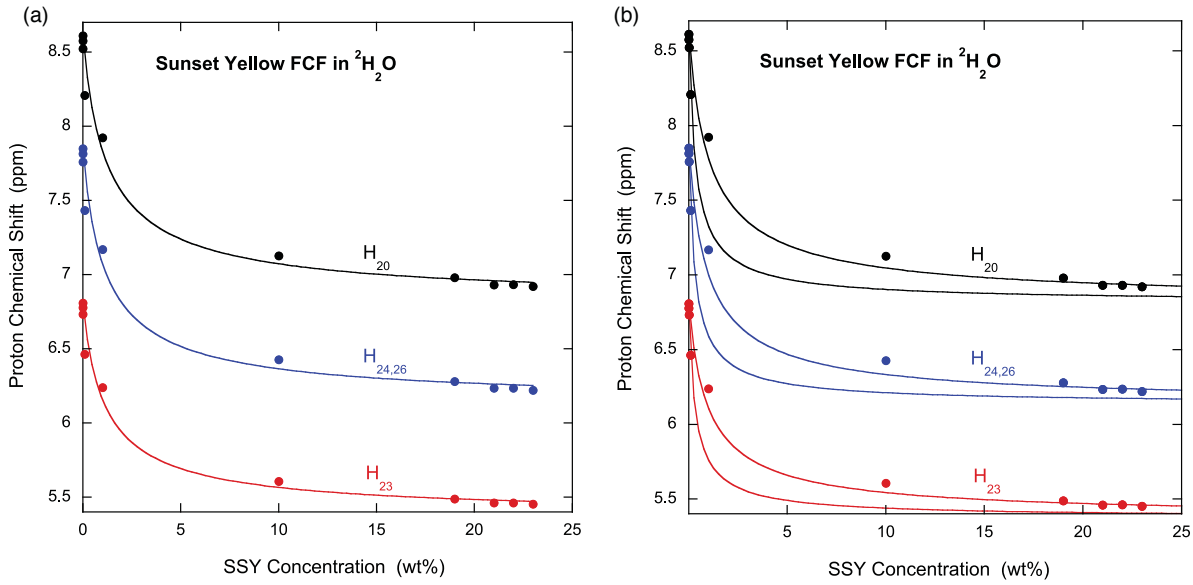


Figure 27. Proton chemical shifts for Sunset Yellow FCF versus a wide range of concentration (data and proton numbering taken from Ref. [65, Table 1]). The isodesmic assembly model, Equation (4) is used to fit the data, with the chemical shift of the molecule fixed at the value given in Table 1. Fits to all of the data are shown in (a). Fits to the lowest and highest four data points with the chemical shifts of the assembly fixed at the best fit values found in (a) are shown in (b).

larger stacking free energy change for SSY, namely about 11 $k_BT$.[66] This finding has become more interesting as a result of crystal structure determination of a guanidinium salt of SSY and theoretical simulations using molecular dynamics, metadynamics, and quantum chemical computations.[67] The pairwise interactions in the disordered crystal structure correspond quite well to the stereochemistry of SSY molecules in solution and the simulations yield a value for the stacking free energy change of a little over 11 $k_BT$ . Perhaps more important, the calculations reveal that lateral shifts of molecules in the assembly form quite readily, a proposal made earlier to explain why measurements of the assembly length might give results lower than the actual value.[48] The simulation also demonstrated that another possible stacking defect, a Y-junction, does not occur much at all.

### *6.5. Other measurements*

Other experimental methods have been used for the study of the assembly process in chromonic liquid crystals, but much more sparingly. Magnetic birefringence studies done on DSCG shortly after its unusual assembly properties were discovered are revealing. Such a measurement involves measuring the birefringence in the isotropic phase as a function of applied magnetic field. The slope of the birefringence versus magnetic field squared plot gives the Cotton–Mouton constant. For DSCG solutions in the 0.3 to 1.3 wt% range, the Cotton–Mouton constant appears to be roughly linear, with an intercept consistent with zero.[68] A more recent magnetic birefringence measurement involves several compounds, higher magnetic fields, and varying temperature. By varying the temperature in the isotropic phase just above the isotropic–nematic coexistence region, the assembly process and nematic correlations can be investigated through measurements of the Cotton–Mouton constant. For three of the compounds investigated, the data follow what one would expect from basic theoretical ideas, but this is not true for DSCG, again pointing out the result of many different experiments that the assembly process in DSCG at concentrations approaching that necessary for formation of the liquid crystal phase is unique.[69]

Rheology is also useful in investigating the assembly process. The zero shear viscosity of PIC at 25°C increases sharply by 5 orders of magnitude over the same concentrations at which the narrow red-shifted absorption band indicating assembly formation appears.[70] A rise in the dynamical viscosity of SSY is observed at concentrations where NMR diffusion measurements indicate that almost all of the molecules are in assemblies.[66] The data for PIC and SSY are plotted in Figure 28. Clearly, these two systems belong to the two different classes of chromonic liquid crystals. PIC forms complex assemblies at low concentrations with no isotropic–liquid crystal two-phase region observed.[70] SSY forms simple assemblies of stacked molecules at high concentrations and a wide two-phase region is present. Also the assembly process in PIC has a threshold, whereas the assembly process in SSY is isodesmic. These differences are apparent in the different rheological properties observed for these two systems.

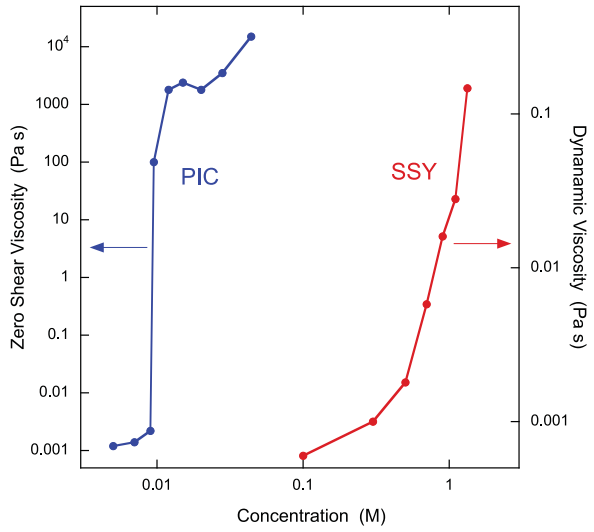


Figure 28. Viscosity measurements for two chromonic liquid crystals. The PIC data are taken from Ref. [70] and the SSY data are taken from Ref.[66]

### *6.6. Kinetics measurements*

Kinetics experiments can be extremely useful in revealing the details of many assembly processes, for example, protein aggregation, amyloid formation, actin polymerization, and microtubule assembly. Surprisingly, there is very little work on the kinetics of assembly in dye systems that form liquid crystal phases. The assembly of neutral tetrakis-4-sulfonatophenylporphine can be initiated at very low concentration by conversion to the diacid form ($H_4TPPS_4^{2-}$) following the addition of HCl. This system precipitates at concentrations too low to form the liquid crystal phase. The kinetics can be monitored by absorption at the proper wavelength, revealing a sigmoidal-shaped profile over thousands of seconds with a significant incubation period. If the same solution is "seeded" by adding a small amount of concentrated $H_4TPPS_4^{2-}$ solution, the incubation period disappears and the profile follows a simple exponential.[71] Merocyanine dyes assemble into helical nanorods, a process that can be monitored by absorption and circular dichroism measurements. Assembly is initiated by the addition of methylcyclohexane and the process takes many thousands of seconds.[72] Similar experiments can be done with squarine dyes by addition of a poor solvent such as acetonitrile. The profile obeys second-order kinetics and takes thousands of seconds.[73] The formation of fibers by a shape-persistent macrocycle can be initiated by a change in temperature and monitored by measuring the magnetic birefringence. This process can take many hours to complete.[74] Finally, PIC molecules can be induced to assemble at low concentration if polyvinylsulfonate is present as a template. The process is slow (thousands of seconds) and the non-sigmoidal profile can be fit nicely by a model in which the rate constant is time-dependent due to the self-similar nature of the assemblies.[71]

The most simple type of assembly process for chromonic liquid crystals is isodesmic assembly into simple stacks of molecules as occurs for SSY. However, the assembly and disassembly processes in this case are much

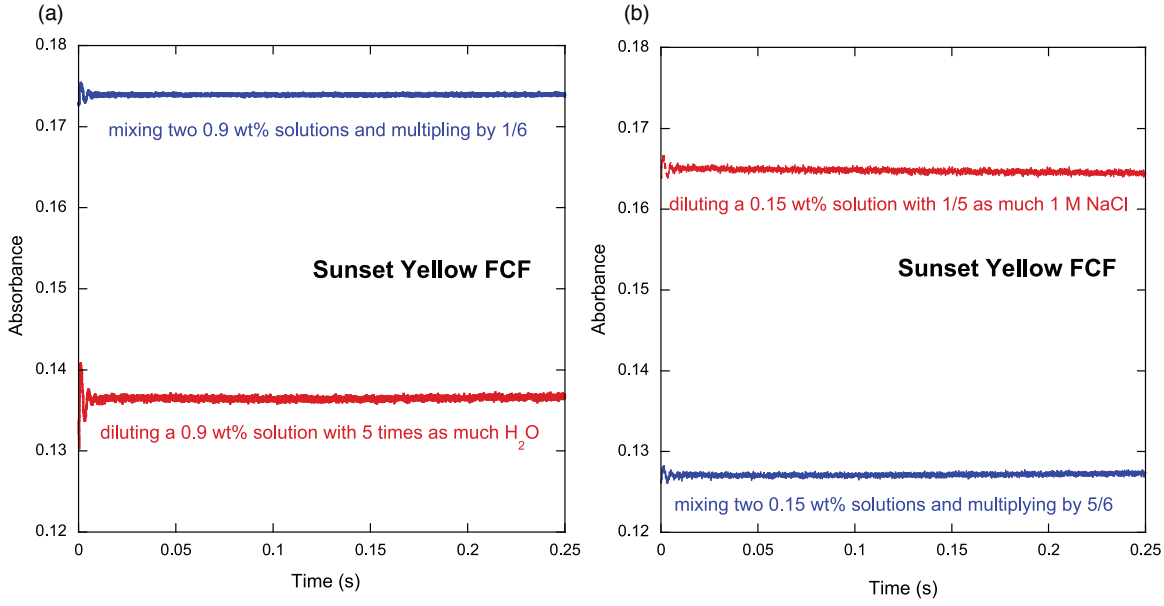


Figure 29. Kinetics of assembly and disassembly for Sunset Yellow FCF (from Ref. [75]). The absorption at 560 nm is monitored for a 1 mm path length cell as an SSY solution is diluted. (a) A 0.9 wt% SSY solution is diluted with 5 times as much water. The top trace is the result of mixing two 0.9 wt% SSY solutions and multiplying by $\frac{1}{6}$. The bottom trace is the actual experimental kinetic result. (b) A 0.15 wt% SSY solution is diluted with $\frac{1}{5}$ as much 1 M NaCl solution. The bottom trace is the result of mixing two 0.15 wt% SSY solutions and multiplying by $\frac{5}{6}$. The top trace is the actual experimental kinetic result.

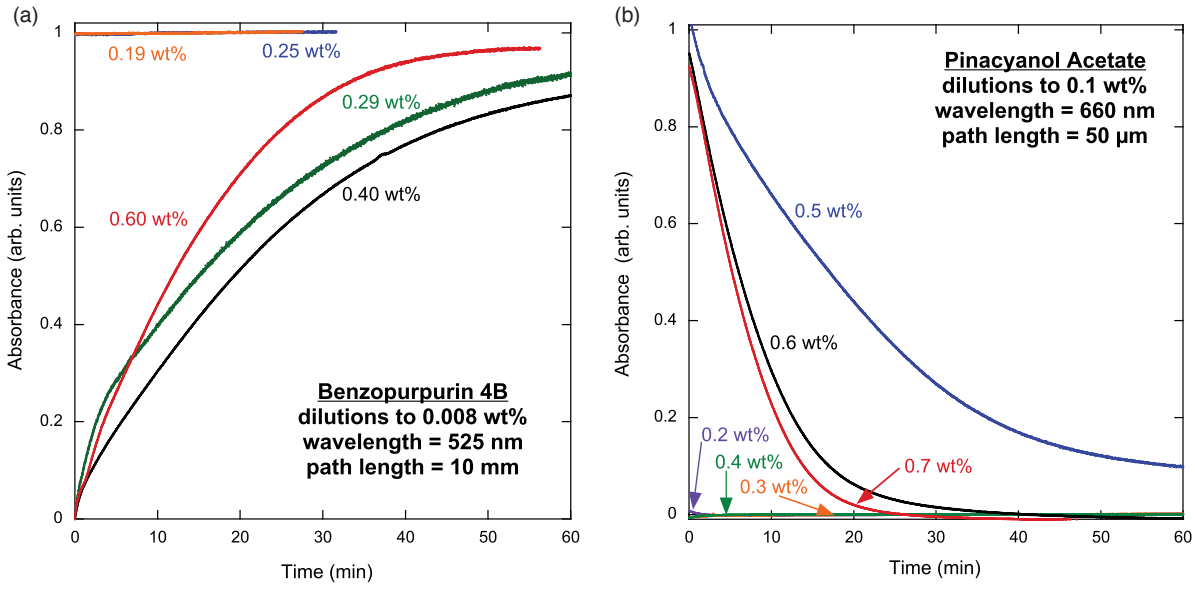


Figure 30. Kinetics of disassembly for (a) benzopurpurin 4B and (b) pinacyanol acetate (from Refs. [76] and [54]). No complex assemblies are present in the 0.19 and 0.25 wt% solutions of benzopurpurin 4B and the 0.2, 0.3, and 0.4 wt% solutions of pinacyanol acetate. For higher concentrations, dilution to a low concentration causes these complex assemblies to disassemble.

faster than for the systems that form more complicated assemblies. One of the most common ways to study kinetics is a stopped-flow apparatus. When a sample of SSY at a concentration well below the liquid crystal phase is investigated using such an apparatus with a dead time of 1 ms, one finds that the process is complete within the dead time. These data are shown in Figure 29, where a 0.9 wt% SSY solution is diluted with 5 times as much water and a 0.15 wt% SSY solution is diluted with $\frac{1}{5}$ as much 1 M NaCl solution.[75] Two kinetic traces are shown on each of the graphs: one is the kinetic trace when mixing two 0.9 or 0.15 wt% SSY solutions multiplied by $\frac{1}{6}$ or $\frac{5}{6}$, respectively, to get the absorption after mixing but before any assembly or disassembly occurs, and the other is the kinetic trace after the actual dilution. If the kinetics were slower, one would observe a trace starting from the scaled undiluted trace and approaching the actual observed trace. The fact that the actual trace is flat at the value expected after the process is complete signifies that the assembly process in SSY is complete in less than 1 ms. Similar fast kinetics are observed for low concentrations of DSCG.

The kinetics of the assembly and disassembly processes are slower for the formation of more complex assemblies in systems that form a liquid crystal phase at low concentrations. The most extensively studied material is IR-806, in which both processes take place on the order of a second.[52] In this case, stopped-flow experiments show quite clearly that there is a threshold to the process because disassembly experiments do not reveal any change unless the starting concentration is high enough and assembly experiments do not reveal any change unless the concentration of the added salt solution is high enough. Similar experiments on benzopurpurin 4B and pinacyanol acetate reveal both slow kinetics and a threshold. Figure 30(a) demonstrates that there is no change if the starting concentration of Benzopurpurin 4B is less than 0.29 wt%.[76] Likewise, Figure 30(b) shows that there is no change if the starting concentration of pinacyanol acetate is less than 0.5 wt%.[54]

In addition, the experiments on IR-806 show that if the starting concentration is less than the threshold for the formation of complex assemblies, dilution with a salt solution causes complex assemblies to form, but only if the concentration of the added salt solution is high enough.[52] The same is true for pinacyanol acetate, as can be seen from Figure 31.[54] The starting concentration is 0.11 wt%, well below the threshold for complex assembly formation. Addition of one-tenth as much salt solution causes a change in the absorbance only if the concentration of NaCl is higher than 35 mM.

It is interesting to compare the results of kinetics experiments with some of the assembly models. A close look at the dilution experiments for IR-806 shows that the kinetics profile at first changes quite rapidly and then changes much more slowly. This can be seen in Figure 32, in which the change during the first fraction of a second is much more rapid that for later times.[53] This is exactly what the nucleation and growth model predicts if the disassembly of nuclei is much slower than the breakup of larger assemblies into nucleus-size assemblies. The assemblies are larger than a nucleus, so the first part of the disassembly process is when the assemblies break down into sizes close to the nucleus size causing the breakup of the nuclei

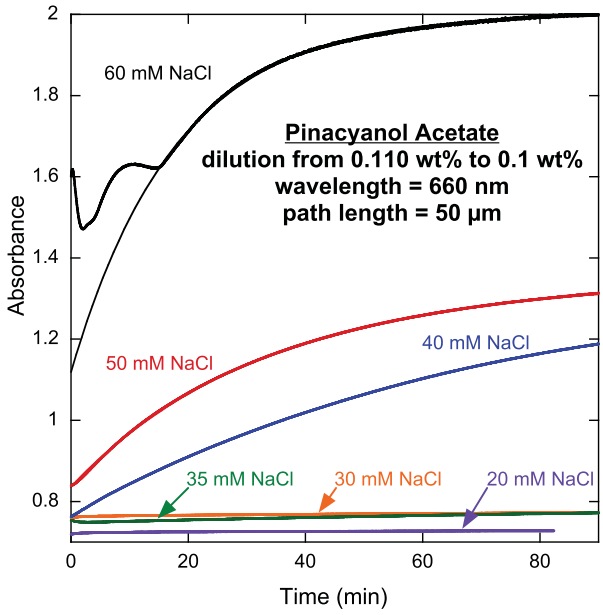


Figure 31. Assembly kinetics for pinacyanol acetate using a hand-mixing method with a dead time of a few minutes (from Ref. [54]). The starting concentration is 0.11 wt% and addition of one-tenth as much salt solution brings the final pinacyanol acetate concentration down to 0.1 wt%. Only for added NaCl solutions above 35 mM do complex assemblies form resulting in a change in the absorbance. These can be fitted to an simple exponential curve (visible only for the 60 mM data below 15 minutes), with rate constants that increase with the NaCl concentration. All experiments with the 60 mM NaCl solution show an unusual profile at the beginning.

to proceed faster. Then more slowly the nuclei break down into individual entities, which in the case of IR-806 are the assemblies that form due to the isodesmic process at lower concentrations or higher temperatures.[52] Also shown in Figure 32 is the prediction of the nucleation and growth model using parameters chosen to qualitatively agree with the experimental data and an exponential fit to the data for reference purposes.

The nucleation and growth model also does a nice job describing the kinetics of IR-806 when a small amount of salt solution is added to induce formation of the complex assemblies. This can be done with an IR-806 solution with a concentration below the threshold for complex assembly formation.[52] As can be seen from Figure 33, proper selection of the parameters in the nucleation and growth model yields a kinetics profile very similar to what is obtained in an experiment.[53] It is interesting to look at the model calculation that follows the data. Although the threshold is experimentally and theoretically very sharp, a small number of complex assemblies are present just below the threshold. For example, for the model calculation that follows the experimental data of Figure 33, the fraction of intermediate assemblies in large assemblies is on the order of $10^{-5}$ and this affects the slope of the kinetics profile at the earliest times.

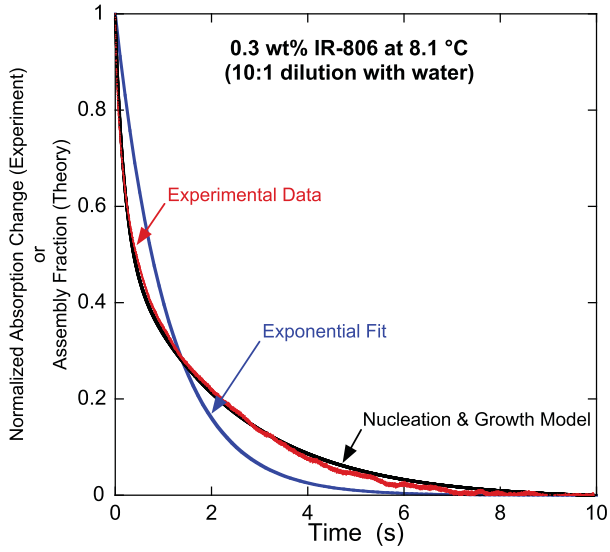


Figure 32. Kinetics due to a 10:1 water/IR-806 solution dilution for a 0.3 wt% IR-806 solution at 8.1°C using absorption at 870 nm (from Ref. [53]). The parameters used for the nucleation and growth model are selected to give a curve similar to the experimental data: $C_T = 1$ wt%, $N = 10$,$k_{N+} = 0.5\,\mathrm{s}^{-1}\,\mathrm{wt\%}^{-9}$, $k_{N-} = 0.5\,\mathrm{s}^{-1}$, $k_+ = 120\,\mathrm{s}^{-1}\,\mathrm{wt\%}^{-1}$, and $k_- = 70\,\mathrm{s}^{-1}$. An exponential fit to the data is also shown for reference.

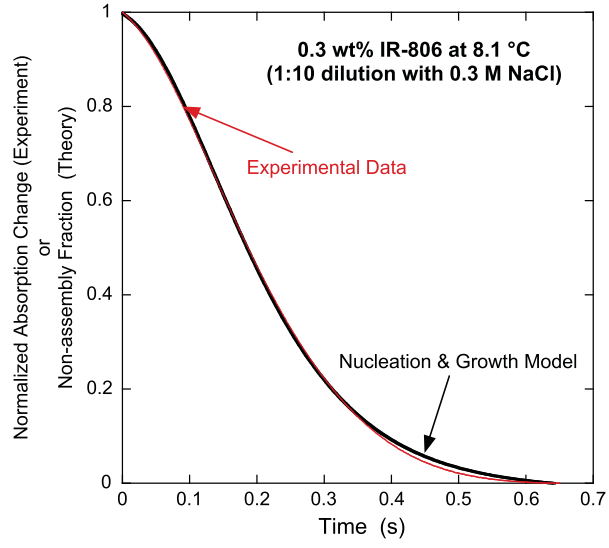


Figure 33. Kinetics due to the addition of NaCl in a 1:10 ratio of NaCl/IR-806 solution from absorption measurements at 560 nm and a temperature of 29.7°C (from Ref. [53]). The concentration or IR-806 is initially 0.3 wt% and the concentration of the added NaCl solution is 0.3 M. The parameters used for the nucleation and growth model are selected to give a curve similar to the experimental data: $C_T = 0.5$ wt%, $N = 8$, $k_{N+} = 0.25\,\mathrm{s}^{-1}\,\mathrm{wt\%}^{-9}$, $k_{N-} = 125\,\mathrm{s}^{-1}$, $k_+ = 14000\,\mathrm{s}^{-1}\,\mathrm{wt\%}^{-1}$, and $k_- = 14000\,\mathrm{s}^{-1}$, initially, with $k_{N+}$ and $k_+$ jumping by a factor of 2.5 to simulate salt addition.

### 6.7. *Solvent dependence*

The fact that chromonic liquid crystal molecules can be induced to assemble by the addition of salt demonstrates

that solvent conditions play a very strong role in determining the assembly behavior. There has been very little research done on the effect of changing solvent conditions on the nature of the assembly process, including quantitative measurements of equilibrium and kinetic constants. Much more attention has been paid to how different solvent conditions affect the stability of the various liquid crystal phases. Ref. [16] summarizes the dependence on solvent conditions by discussing three effects: (1) ionic additives, (2) non-ionic additives, and (3) pH. Ref. [48] goes into more detail on ionic additives, showing that at lower concentrations NaCl, $MgCl_2$, and $MgSO_4$ (in order of increasing strength) raise the isotropic–nematic transition temperature for SSY and attribute it to the screening of the charged sulfonate groups, thus effectively increasing the growth equilibrium constant and therefore the stacking free energy change. The addition of the neutral polymer polyethylene glycol (PEG) to SSY solutions also tends to make the liquid crystal phases more stable due to the separation into SSY-rich regions and PEG-rich regions.[77] At lower concentrations, it is likely that PEG acts as a depletion agent, forcing the SSY molecules into a smaller volume, effectively increasing the SSY volume fraction. The effect is similar to increasing the stacking free energy change. Similar effects are found for DSCG and some water-soluble polymers, indicating that the depletion effect due to the presence of these polymers is quite general.[78] Increasing the pH of the solution has the opposite effect. At high pH, the molecules carry more charge on average, increasing the electric repulsion between them. This is seen as a decrease in the degree of SSY assembly as the pH is increased,[79] demonstrating that high pH has the effect of reducing the stacking free energy change. A reduction in the stability of the liquid crystal phase also results.[48,80]

It should be kept in mind that different solvent conditions can change the structure of the assemblies that are formed. While adding modest amounts of NaCl to IR-806 solutions normally produces a spectral change identical to an increase in the IR-806 concentration,[52] such is not always the case. If the IR-806 concentration is low, adding NaCl can lead to spectra that are not similar to the spectra observed at any IR-806 concentration without added NaCl.

### *6.8. Imaging the assemblies*

Although a wealth of evidence is available for the formation of both simple and complex assembly structures, there is nothing better than to actually image them. The amount of research in this area is not extensive, but results in the past few years forecast important advances in the near future.

The most common technique for imaging the assemblies is transmission electron microscopy after rapid freezing of the solution (cryo-TEM). In such an experiment, a drop of solution is put on an open grid, the excess solution is blotted off, and the grid is quickly plunged into a cryogenic bath such as liquid ethane. The ultrafast cooling achieves artifact-free thermal fixation of the aqueous solution, thus preventing crystallization of the water and rearrangement of the assemblies. The grid is kept at cryogenic temperatures as it is transferred to a transmission electron microscope and remains at that temperature during exposure to a low-intensity X-ray beam. More details on cryo-TEM, including variants on the procedure just described, are contained in a recent paper reviewing the experiments on both thermotropic and lyotropic liquid crystals.[25]

When such an experiment is performed on PIC, one can observe long, rod-like assemblies with a diameter of $2.3 \pm 0.2$ nm with lengths averaging 300–400 nm.[81] When NaCl is added to the PIC solution, a network superstructure of isolated fibers and complex fiber bundles is observed. Dilution of one of these samples reveals isolated thread-like assemblies with a diameter of 2.3 nm.[82] The situation appears to be quite different for pinacyanol chloride. Cryo-TEM experiments on freshly prepared samples show tubular assemblies with a single-layer wall thickness of about 2.5 nm and an outer diameter of roughly 6.5 nm. These assemblies transform to a different type of assembly over many weeks. These new assemblies are approximately 9 nm wide and consist of stacked pairs of ribbons that eventually form tape-like ribbons.[24] Cryo-TEM experiments performed on DSCG reveal parallel assemblies in both the isotropic and nematic phases. The distance between assemblies averages roughly 4.2 nm and their lengths are in the 25–80 nm range. The separation nicely matches the results of X-ray diffraction investigations, although the lengths are a bit longer. The higher

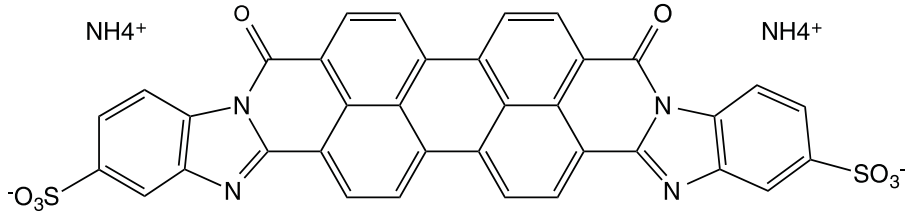


Figure 34. Molecular structure of Violet 20.

viscosity of SSY solutions makes cryo-TEM more difficult, but it is still possible. Rod-like assemblies are visible with separations between 2.0 and 2.4 nm, which is consistent with the results of X-ray diffraction studies.[25]

Since chromonic liquid crystals can be spread on a substrate and allowed to dry, imaging the assemblies in the resulting thin film is also possible. An atomic force microscopy study of Violet 20, the structure of which is shown in Figure 34, demonstrates that oriented monolayers are achieved through a shear deposition method in the nematic phase. The images of the assemblies show they are 1–2 nm wide, 1–2 nm tall, and 1–2 nm apart.[83]

## 7. Conclusions

The study of chromonic liquid crystal systems is both challenging and unique. The basic components are molecular assemblies, a property of widespread importance across an array of matter. The basic components spontaneously order both orientationally and positionally, a trait shared with many other systems. Possessing both qualities simultaneously obviously makes for complicated behavior, but it also allows for a huge array of phenomena. Other lyotropic liquid crystal systems are in many ways quite similar, but the combination of attractive interactions between the aromatic parts of molecules and the amphiphilic character of the molecules is unique. There is a great deal to be learned about chromonic liquid crystals, and the chances are very good that one of their unique properties will be the feature that allows for unique applications. One of the many aspects of chromonic liquid crystals that must be understood to make progress is the nature of the assembly process. Much has already been learned, but much more waits to be discovered.

## Acknowledgments

The authors also thank Heinrich Roder and Ming Xu of the Fox Chase Cancer Center (Philadelphia, PA) for allowing the use of the SX20 stopped-flow spectrophotometer.

## Disclosure statement

No potential conflict of interest was reported by the authors.

## Funding

Partial support of this research from the donors of the American Chemical Society Petroleum Research Fund is gratefully acknowledged, along with support from the Howard Hughes Medical Institute and the REU Program at the Laboratory for Research in the Structure of Matter at the University of Pennsylvania.

## Note

1. This assumes the element of phase space used to calculate the external degrees of freedom is set equal to the molecular volume.

## References

[1] Sandquist H. Anisotropic aqueous solution. Ber Dtsch Chem Ges. 1915;48:2054–2055.
[2] Jelley EE. Spectral absorption and fluorescence of dyes in the molecular state. Nature. 1936;138:1009–1010.
[3] Jelley EE. Molecular, nematic and crystal states of i: i-diethyl-cyanine chloride. Nature. 1937;139:631–632.
[4] Schiebe G. Über die veränderlichkeit der absorptionsspektren in lösungen und die nebenvalenzen als ihre ursache. Angew Chem Int Ed Engl. 1937;50:212–219.
[5] Hartshorne NH, Woodward GD. Mesomorphism in the system disodium chromoglycate-water. Mol Cryst Liq Cryst. 1973;23:343–368.
[6] Lydon JE. New models for the mesophases of disodium cromoglycate (INTAL). Mol Cryst Liq Cryst. 1980;64:19–24.
[7] Jones F, Kent DR. Aggregation and lyotropic mesophase formation in anionic dye solutions. Dyes Pigments. 1980;1:39–48.
[8] Attwood TK, Lydon JE. Lyotropic mesophase formation by anti-asthmatic drugs. Mol Cryst Liq Cryst. 1984;108:349–357.
[9] Perahia D, Wachtel EJ, Luz Z. NMR and X-ray studies of the chromonic lyomesophases formed by some xanthone derivatives. Liq Cryst. 1991;9:479–492.
[10] Tiddy GJT, Mateer DL, Ormerod AP, Harrison WJ, Edwards DJ. Highly ordered aggregates in dilute dye-water systems. Langmuir. 1995;11:390–393.
[11] Lydon J. Chromonics. In: Demus D, Goodby J, Gray GW, Spiess H-W, Vill V, editors. Handbook of liquid crystals. Vol. 2B. New York (NY): Wiley-VCH; 1998. p. 981–1007.
[12] TamChang SW, Huang L. Chromonic liquid crystals: properties and applications as functional materials. Chem Commun. 2008;2008:1957–1967.
[13] Chen Z, Lohr A, Saha-Moller CR, Wurthner F. Self-assembled $\pi$-stacks of functional dyes in solution: structural and thermodynamic features. Chem Soc Rev. 2009;38:564–584.
[14] Lydon J. Chromonic review. J Mater Chem. 2010;20:10071–10099.
[15] Lydon J. Chromonic liquid crystalline phases. Liq Cryst. 2011;38:1663–1681.
[16] Park HS, Lavrentovich OD. Lyotropic Chromonic liquid crystals: emerging applications. In: Li Q, editor. Liquid crystals beyond displays: chemistry, physics, and applications. Hoboken (NJ): John Wiley & Sons; 2012. p. 449–484.
[17] Lydon J. Chromonic liquid crystals. In: Goodby JW, Collings PJ, Kato T, Tschierske C, Gleeson HF, Raynes P, editors. Handbook of liquid crystals. Vol. 6. Weinheim: Wiley-VCH; 2014. p. 439–483.
[18] Stegemeyer H, Stockel F. Anisotropic structures in aqueous solutions of aggregated pseudoisocyanine dyes. Ber Bunsenes Phys Chem. 1996;100:9–14.
[19] Harrison WJ, Mateer DL, Tiddy GJT. Liquid-crystalline j-aggregates formed by aqueous ionic cyanine dyes. J Chem Phys. 1996;100:2310–2321.
[20] Bykov VA, Sharimanov YG, Mrevlishvili GM, Mdzinarashvili TD, Metreveli NO, Kakabadze GR. Phase diagram for aqueous solutions of benzopurpurin 4b organic dye and effect of water on stabilization of lyotropic liquid-crystalline structures. Mol Matter. 1992;1:73–83.
[21] McKitterick CB, Erb-Satullo NL, LaRacuente ND, Dickinson AJ, Collings PJ. Aggregation properties of the

chromonic liquid crystal benzopurpurin 4b. J Phys Chem B. 2010;114:1888–1896.
[22] Rodriguez-Abreu C, Torres CA, Tiddy GJT. Chromonic liquid crystalline phases of pinacyanol acetate: characterization and use as templates for the preparation of mesoporous silica nanofibers. Langmuir. 2011;27:3067–3073.
[23] Mills EA, Regan MH, Stanic V, Collings PJ. Large assembly formation via a two-step process in a chromonic liquid crystal. J Phys Chem B. 2012;116:13506–13515.
[24] von Berlepsch H, Ludwig K, Bottcher C. Pinacyanol chloride forms mesoscopic H- and J-aggregates in aqueous solution – a spectroscopic and cryo-transmission electron microscopy study. Phys Chem Chem Phys. 2014;16: 10659–10668.
[25] Gao M, Kim Y, Zhang C, Borshch V, Zhou S, Park H, Jakli A, Lavrentovich O, Tamba M, Kohlmeier A, Mehl G, Weissflog W, Studer D, Zuber B, Gnagi H, Lin F. Direct observation of liquid crystals using cryo-tem: specimen preparation and low-dose imaging. Microsc Res Tech. 2014;77:754–772.
[26] Martin RB. Comparisons of indefinite self-association models. Chem Rev. 1996;96:3043–3064.
[27] Gelbart WM, Ben-Shaul AJ. The "new" science of "complex fluids". Phys Chem. 1996;100:13169–13189.
[28] Smulders MMJ, Nieuwenhuizen MML, deGreef TFA, vanderSchoot P, Schenning APHJ, Meijer EW. How to distinguish isodesmic from cooperative supramolecular polymerisation. Chem Eur J. 2010;16:362–367. (Supporting Information).
[29] van der Schoot P. Theory of supramolecular polymerization. In: Ciferri A, editor. Supramolecular polymers. 2nd ed. Boca Raton (FL): CRC Press; 2005. p. 77–106.
[30] Morris AM, Watzky MA, Finke RG. Protein aggregation kinetics, mechanism, and curve-fitting: a review of the literature. Biochim Biophys Acta. 2009;1794:375–397.
[31] Cohen SIA, Vendruscolo M, Dobson CM, Knowles TPJ. The kinetics and mechanisms of amyloid formation. In: Otzen DE, editor. Amyloid fibrils and prefibrillar aggregates: molecular and biological properties. Weinheim: Wiley-VCH; 2013. p. 183–209.
[32] Michaels TCT, Knowles TPJ. Mean-field master equation formalism for biofilament growth. Am J Phys. 2014;82: 476–483.
[33] Taylor MP, Herzfeld J. A model for nematic and columnar ordering in a self-assembling system. Langmuir. 1990;6:911–915.
[34] Taylor MP, Herzfeld J. Shape anisotropy and ordered phases in reversibly assembling lyotropic systems. Phys Rev A. 1991;43:1892–1905.
[35] Taylor MP, Herzfeld J. Liquid-crystal phases of self-assembled molecular aggregates. J Phys Condens Matter. 1993;5:2651–2678.
[36] Cates ME, Candau SJ. Statics and dynamics of worm-like surfactant micelles. J Phys Condens Matter. 1990;2: 6869–6892.
[37] Edwards RG, Henderson JR, Pinning RL. Simulation of self-assembly and lyotropic liquid crystal phases in model discotic solutions. Mol Phys. 1995;86:567–598.
[38] Maiti PK, Lansac Y, Glaser MA, Clark NA. Isodesmic self-assembly in lyotropic chromonic systems. Liq Cryst. 2002;29:619–626.
[39] Lu XJ, Kindt JT. Monte Carlo simulation of the self-assembly and phase behavior of semiflexible equilibrium polymers. J Chem Phys. 2004;120:10328–10338.
[40] Kuriabova T, Betterton MD, Glaser MA. Linear aggregation and liquid-crystalline order: comparison of monte carlo simulation and analytic theory. J Mater Chem. 2010;20: 10366–10383.
[41] Mohanty S, Chou S-H, Brostrom M, Aguilera J. Predictive modeling of self assembly of chromonics materials. Mol Simul. 2006;32:1179–1185.
[42] Chami F, Wilson MR. Molecular order in a chromonic liquie crystal: a molecular simulation study of the anionic axo dye sunset yellow. J Am Chem Soc. 2010;132: 7794–7802.
[43] Akinshina A, Walker M, Wilson MR, Tiddy GJT, Masters AJ, Carbone P. Thermodynamics of the self-assembly of non-ionic chromonic molecules using atomistic simulations. The case of tp6eo2m in aqueous solution. Soft Matter. 2014;11:680–691.
[44] Walker M, Masters AJ, Wilson MR. Self-assembly and mesophase formation in a non-ionic chromonic liquid crystal system: insights from dissipative particle dynamics simulations. Phys Chem Chem Phys. 2014;16: 23074–23081.
[45] Dickinson AJ, LaRacuente ND, McKitterick CB, Collings PJ. Aggregate structure and free energy changes in chromonic liquid crystals. Mol Cryst Liq Cryst. 2009;509: 9/[751]–20/[762].
[46] Collings PJ, Dickinson AJ, Smith EC. Molecular aggregation and chromonic liquid crystals. Liq Cryst. 2010;37: 701–710.
[47] Agra-Kooijman DM, Singh G, Lorenz A, Collings PJ, Kitzerow H-S, Kumar S. Columnar molecular aggregation in the aqueous solutions of disodium cromoglycate. Phys Rev E. 2014;89:062504-1–062504-6.
[48] Park H-S, Kang S-W, Tortora L, Nastishin Y, Finotello D, Kumar S, Lavrentovich OD. Self-assembly of lyotropic chromonic liquid crystal sunset yellow and effects of ionic additives. J Phys Chem B. 2008;112:16307–16319.
[49] Joshi L, Kang S-W, Agra-Kooijman DM, Kumar S. Concentration, temperature, and pH dependence of sunset yellow aggregates in aqueous solutions: an X-ray investigation. Phys Rev E. 2009;80:041703-1–041703-8.
[50] Regan MH, Collings PJ. Unpublished raw data. 2015.
[51] Neumann B, Huber K, Pollmann P. A comparative experimental study of the aggregation of acid red 266 in aqueous solution by use of $^{19}$F-NMR, UV/vis spectroscopy and static light scattering. Phys Chem Chem Phys. 2000;2: 3687–3695.
[52] Mercado BR, Nieser KJ, Collings PJ. Cooperativity of the assembly proces in a low concentration chromonic liquid crystal. J Phys Chem. 2014;118:13312–13320.
[53] Mercado BR, Collings PJ. Unpublished raw data. 2015.
[54] Goldstein JN, Collings PJ. Unpublished raw data. 2015.
[55] Jonkheijm P, van der Schoot P, Schenning APHJ, Meijer EW. Probing the solvent-assisted nucleation pathway in chemical self-assembly. Science. 2006;313: 80–83.
[56] Neumann B. On the aggregation behavior of pseudoisocyanine chloride in aqueous solution as probed by UV/vis spectroscopy and static light scattering. J Phys Chem. 2001;105:8268–8274.
[57] Nastishin YuA, Liu H, Shiyanovskii SV, Lavrentovich OD, Kostko AF, Anisimov MA. Pretransitional fluctuations in the isotropic phase of a lyotropic chromonic liquid crystal. Phys Rev E. 2004;70:051706-1–051706-9.
[58] Bertrand CE, Linegar KL, Kostko AF, Anisimov MA. Multiscale dynamics of pretransitional fluctuations in the isotropic phase of a lyotropic liquid crystal. Phys Rev E. 2009;79:041704-1–041704-13.

[59] Yu LJ, Saupe A. Deuteron resonance of $D_2O$ of nematic disodium cromoglycate-water systems. Mol Cryst Liq Cryst. 1982;80:129–134.
[60] Perahia D, Goldfarb D, Luz Z. Sodium-23 NMR in the lyomesophases of disodiumcromoglycate. Mol Cryst Liq Cryst. 1984;108:107–123.
[61] Hamada K, Take S, Iijima T, Amiya S. Effects of electrostatic repulsion on the aggregation of azo dyes in aqueous solution. J Chem Soc Faraday Trans. 1986;82:3141–3148.
[62] Hamada K, Mitshuishi M, Ohira M, Miyazaki K. Positional effects of a trifluoromethyl group on the aggregation of azo dyes in aqueous solutions. J Chem Phys. 1993;97: 4926–4929.
[63] Perahia D, Luz Z, Wachtel EJ, Zimmermann H. NMR and X-ray diffraction of the 7,7'-disodiumcromoglycate-water lyomesophases. Liq Cryst. 1987;2:473–489.
[64] Edwards DJ, Jones JW, Lozman O, Ormerod AP, Sintyureva M, Tiddy GJT. Chromonic liquid crystal formation by edicol sunset yellow. J Phys Chem B. 2008;112:14628–14636.
[65] Jones JW, Lue L, Ormerod AP, Tiddy GJT. The influence of sodium chloride on the self-association and chromonic mesophase formation of edicol sunset yellow. Liq Cryst. 2010;37:711–722.
[66] Renshaw MP, Day IJ. NMR characterization of the aggregation state of the azo dye sunset yellow in the isotropic phase. J Phys Chem. 2010;114:10032–10038.
[67] Xiao W, Hu C, Carter DJ, Nichols S, Ward MD, Raiteri P, Rohl AL, Kahr B. Structural correspondence of solution, liquid crystal, and crystalline phases of the chromonic mesogen sunset yellow. Cryst Growth Des. 2014;14: 4166–4176.
[68] Champion JV, Meeten GH. Conformation of soidum cromolyn in aqueous solution using light scattering and magnetic birefringence. J Pharm Sci. 1973;62:1589–1595.
[69] Ostapenko T, Nastishin YA, Collings PJ, Sprunt SN, Lavrentovich OD, Gleeson JT. Aggregation, pretransitional behavior, and optical properties in the isotropic phase of lyotropic chromonic liquid crystals studied in high magnetic fields. Soft Matter. 2013;9:9487–9498.
[70] Rehage H, Platz G, Struller B, Thunig C. Reheological properties of dye assemblies. Tenside Surf Det. 1996;33: 242–248.
[71] Pasternack RF, Fleming C, Herring S, Collings PJ, dePaula J, DeCastro G, Gibbs EJ. Aggregation kinetics of extended porphyrin and cyanine dye assemblies. Biophys J. 2000;79:550–560.
[72] Lohr A, Lysetska M, Wurthner F. Supramolecular stereomutation in kinetic and thermodynamic self-assembly of helical merocyanine dye nanorods. Angew Chem Int Ed. 2005;44:5071–5074.
[73] Jyothish K, Hariharan M, Ramaiah D. Chiral supramolecular assemblies of a squaraine dye in solution and this films: concentration-, temperature-, and solvent-induced chirality inversion. Chem Eur J. 2007;13:5944–5951.
[74] Gielen JC, Ver Heyen A, Klyatskaya S, Vanderlinden W, Höger S, Maan JC, De Feyter S, Christianen PCM. Aggregation kinetics of macrocycles detected by magnetic birefringence. J Am Chem Soc. 2009;131:14134–14135.
[75] Hamilton EJ, Collings PJ. Unpublished raw data. 2015.
[76] Nieser KJ, Collings PJ. Unpublished raw data. 2015.
[77] Park H-S, Kang S-W, Tortora L, Kumar S, Lavrentovich OD. Condensation of self-assembled lyotropic chromonic liquid crystal sunset yellow in aqueous solutions crowded with polyethylene glycol and doped with salt. Langmuir. 2011;27:4164–4175.
[78] Simon KA, Sejwal P, Gerecht RB, Luk Y-Y. Water-in-water emulsions stabilized by non-amphiphilic interactions: polymer-dispersed lyotropic liquid crystals. Langmuir. 2007;23:1453–1458.
[79] Gooding JJ, Compton RG, Brennan CM, Atherton JH. A new electrochemical method for the investigation of the aggregation of dyes in solution. Electroanalysis. 1997;9:759–764.
[80] Tortora L, Park H-S, Antion K, Finetello D, Lavrentovich OD. Lyotropic chromonic liquid crystals as materials for optical and biosensing applications. Proc SPIE. 2007;6487:6487O1-1–6487O1-15.
[81] von Berlepsch H, Böttcher C, Dähne L. Structure of J-aggregates of pseudoisocyanine dye in aqueous solution. J Phys Chem B. 2000;104:8792–8799.
[82] von Berlepsch H, Böttcher C. Network superstructure of pseudoisocyanine *J*-aggregates in aqueous sodium chloride solution revealed by cryo-transmission electron microscopy. J Phys Chem B. 2002;106:3146–3150.
[83] Schneider T, Smith A, Lavrentovich OD. Imaging oriented aggregates of lyotropic chromonic mesogenic dyes by atomic force microscopy. Mat Res Soc Symp. 2001;636:D11.8.1–D11.8.5.